OBSERVATION OF T-ANTIGEN G-QUADRUPLEX DNA HELICASE ACTIVITY AND INHIBITION

THESIS

Presented to the Graduate Council of
Texas State University-San Marcos
in Partial Fulfillment
of the Requirements

for the Degree

Master of SCIENCE

by

Fatemeh Sanjar, B.S.

San Marcos, Texas
August 2011

FAIR USE AND AUTHOR'S PERMISSION STATEMENT

Fair Use

Duplication Permission

DEDICATION

I would like to dedicate my thesis to my always supportive, encouraging, optimistic, and loving parents without whom I would have never made it this far. My father, Fazlollah Sanjar, and mother, Narges Askaribehbahani, deserve more recognition and acknowledgement than I could ever give them. I would also like to dedicate this thesis to my always loving and supportive companion and soul mate, Mike, which has cheered me on every step of the way for the past 2 years.

ACKNOWLEDGEMENTS

I would like to thank all of my committee members, especially Dr. David, for the continuous help and guidance. I would also like to acknowledge Texas State University-San Marcos for the opportunity and facilities to complete a Master's Thesis.

This manuscript was submitted on 07/15/2011

TABLE OF CONTENTS

Page

ACKNOWLEDGEMENTS vi

LIST OF TABLES.. viii

LIST OF FIGURES..... ix

CHAPTER

I. INTRODUCTION..... 1

II. MATERIALS AND METHODS 20

III. RESULTS AND DISCUSSION 37

APPENDIX.....66

REFERENCES.....68

LIST OF TABLES

Page

Table

1. Summary of DNA Sequence 22

2. Comparison of unfolded G-quadruplex DNA formation in the presence of different salt compositions and concentration... 52

3. ATP nucleotide concentration assay for half enzyme activity of T-ag helicase..... 58

4. Inhibition of T-ag helicase activity via DNA binding of Distamycin A 59

5. Inhibition of T-ag helicase activity via DNA binding of TMPyP4..... 61

LIST OF FIGURES

Page

Figure

1. Inhibition of SV40 T-ag G-quadruplex DNA helicase activity by a G-quadruplex binding agent....10

2. Structure of G-quadruplex DNA and Distamycin A....12

3. Structure of TMPyP4....13

4. Structure of Dictyodendrin B....14

5. Structure of Anti-HIV drugs, CS87 and AZT....15

6. Chemical Structure of a perylene diimide (PDI), Tel11....16

7. Strategy for observing T-ag G-quadruplex helicase activity and inhibition....18

8. Duplex DNA binding assay of CS-86 and CS-87molecules....39

9. DNA binding assay of Dicytodendrin B to G-quadruplex DNA....42

10. Inhibition of DNA helicase activity of T-ag through G-quadruplex DNA binding of TMPyP4....46

11. G-quadruplex DNA binding of Distamycin A to inhibit T-ag DNA helicase activity....48

Page

12. Duplex DNA binding of Tel11 and its inhibitory effect on T-ag DNA helicase activity 49

13. Observation of G-quadruplex DNA structure formation at various salt concentrations 51

14. Observation of G-quadruplex DNA structure Formation in ImG4 DNA strand 53

15. T-ag helicase activity in G-quadruplex DNA (ImG4) unwinding from blunt end complementary DNA strand (G4comp1) 55

16. T-ag helicase unwinding of G-quadruplex DNA (ImG4) from its complementary strand (G4comp2) 56

17. Inhibition of T-ag helicase at half enzyme activity by DNA binding of Distamycin A 60

18. Inhibition of T-ag helicase activity via quadruplex DNA binding of TMPyP4 at different concentrations..... 62

CHAPTER I

Introduction

Simian Virus 40 (SV40)

Due to the complexities of eukaryotic factor proteins in recognizing the origin of replication (OR) and the present uncertainty surrounding many eukaryotic origin sequences involved in DNA replication, Simian Virus 40 (SV40) has been used as a model for a deeper understanding of eukaryotic DNA synthesis, proliferation, and cell division (1, 2, 3, 4). In contrast to the genome of higher eukaryotes, SV40 has a defined origin sequence and recruits fewer proteins for pre-initiation complex formation (2). Viral DNA replication of tumor viruses, such as SV40, is comprised of the following series of steps: recognition and binding of the OR by an initiator protein, melting and consequent unwinding of DNA complex, and finally the recruitment and binding of DNA polymerase along with other protein factors (2, 5). In contrast to the multiple and complex regions involved in eukaryotic cell replication, the SV40 genome contains one well-defined OR region (1, 3). The OR of SV40 is 64-bp in length and consists of three distinct functional regions.

Site II, an AT rich domain, and the EP region (1). The Site II region contains 23-bp perfect palindrome repeats of the sequence GAGGC, the EP region exhibits an imperfect palindrome, and the AT rich domain consists of 17 base-pairs (1). Within Site II region, there are four defined initiator protein binding sites: P1, P2, P3, and P4 (2). The GAGGC pentameric sequence located within the Site II region (1, 2) consists of inverted repeats with a 1-bp spacer between each of the repeats (2). The pentameric GAGGC sequence is thought to be flanked by the AT-rich region on one side and the EP region on the other side (2)

Guanine-rich sequences, such as those observed in the OR region of SV40, are capable of adopting quadruplex structures via Hoogsteen hydrogen bonding between guanine bases. These quadruplex structures are characterized by core guanine tetrads and a number of topologies have been identified (6) Guanine rich DNA structures are commonly referred to as G4 DNA (7, 8, 9), four-stranded DNA (10) or G-quadruplex DNA (7, 10, 11, 12, 13). The physiological relevance of quadruplex-forming regions in the SV40 genome is not known but there are an increasing number of similar examples discussed later in the introduction

SV40 Large Tumor Antigen (T-ag)

SV40 encodes a major early oncogenic helicase protein (5, 14), Large Tumor Antigen (T-ag), for its viral DNA replication (4, 5, 14, 15). DNA helicases are ubiquitous enzymes that were first described by Subramanya and colleagues

(16) about twenty years ago through X-ray crystallography experiments (16, 17). During viral DNA replication, this oncoprotein (14) assembles on the SV40 OR as a double hexamer, induces melting of the DNA complex, and initiates the unwinding of viral DNA (4, 5, 15). The hexamer forms two tiers which can rotate relative to each other by connecting α helices to expand/constrict the central channel, creating an "iris" effect (15). As the name implies, upon viral infection SV40 T-ag is involved in transforming infected cells into a continuously dividing state (14). The method by which T-ag successfully overcomes cell cycle checkpoints is thought to be via hindering the function of tumor suppressor proteins, such as p53, which was the first cellular protein discovered to interact with T-ag (14). Viral DNA replication of SV40 and its initiation at the OR depends on the interaction, DNA binding, and helicase activity of its initiator protein, T-ag DNA helicase (2, 3, 15). Previous studies of T-ag helicase activity have revealed its preference for binding to the single-stranded 3'-tail of synthetic DNA substrates (18) and subsequent translocation in the 3' → 5' direction (4, 10, 17).

T-ag is 708 amino acids residues in length and contains three primary functional domains (1, 2). The functional domains of T-ag helicase are the J domain found at the N-terminus, origin of binding domain (OBD), and helicase domain (1, 2). Past X-ray and NMR studies have provided more insight into the structure and function of these domains (1, 19). The J domain consists of the first 82 amino acid residue sequence, which is involved in interaction with chaperone proteins (1). The OBD spans a region of 131 to 260 amino acid residues that is made of a positively charged central channel surrounded by a left-handed

hexamer, and functions in the sequence-specific initiation of DNA replication at the OR (1, 2). The helicase domain is found from amino acid sequence residues 251 to 627 and is formed from three smaller sub-domains: zinc domain (D1), conserved helicase motif (D2), and globular protein domain (D3) (1).

The helicase activity of SV40 T-ag requires the presence of DNA and Mg^{2+} ions for the formation of the ring structure (10, 19) and it requires the presence of ATP nucleotides for stabilization of T-ag structure and proper functioning during DNA replication (1, 10). Studies have shown that the SV40 T-ag hexameric ring structure forms in the presence of ATP, ADP, AMPyNP, or ATPyS (19). In addition to ATP nucleotide binding, proper DNA interaction and binding of the SV40 genome and the accurate assembly of T-ag on P1 and P3 binding sites of Site II region in the OR is necessary (2). The processivity of T-ag during DNA unwinding is enhanced by cooperativity between ATP hydrolysis and DNA binding (19). SV40 T-ag has been shown to unwind both duplex and G-quadruplex DNA complexes (3, 10, 14).

Upon SV40 viral infection of a host cell, T-ag helicase is responsible for the task of transforming the host cell into a state of continuous cell division (14). As one might guess, studies of T-ag binding to regulatory regions of host cell's gene, such as p53, has been shown to cause the occurrence of tumor cells within experimental animals (14). From an evolutionary standpoint, SV40 T-ag is most closely related to another initiator protein, Bovine Papilloma Virus (BPV) E1 (16), with the difference that T-ag is capable of self-assembly on the OR without assistance of matchmaker proteins (2). To grasp the importance of this

class of proteins in cellular function, it is noteworthy to mention that about 1% of all eukaryotic or prokaryotic genes are estimated to encode helicase proteins (19).

Significance of Helicase activity

Mutations of at least six genes encoding helicase proteins have been reported for several human genetic disorders, such as Werner syndrome, Bloom's syndrome, and Xeroderma Pigmentosum (9, 19). Such genetic disorders can lead to other complications including mental retardation, cancer, immunodeficiency, and premature aging (19). To emphasize the significant role of DNA helicases in cell regulation, proliferation, and maintenance, we thus direct our attention to some genetic disorders caused by DNA helicase mutations.

Bloom's syndrome is a recessive genetic disorder caused by mutation in the BLM gene that encodes a 159-kDa helicase protein, which is a member of the RecQ DNA helicase family (8, 9, 19). Due to a higher level of sister chromatid exchanges the absence of BLM helicase greatly increases genetic instability and early onset of malignancy (8, 9). The BLM helicase unwinds G-quadruplex DNA with at least 15 fold preference compared to B-form DNA structure (9).

Werner syndrome is a genetic disorder caused by mutation of the gene encoding WRN helicase (8, 9, 19). Mutation in the WRN helicase results in chromosomal deletions, translocations (9), and premature aging accompanied by rare malignancies, such as sarcoma (8, 9). Mutations detected in another human RecQ helicase, FANCJ helicase, have been found in individuals suffering from

Fanconia Anemia group J (FA-J) and early onset of breast cancer (7). FANCJ helicase appears to be critical in repair of inter-strand DNA cross linking (ICL) and the timely progression of the cell cycle into S phase (7).

The hallmark of most DNA helicase functional deficiencies is that genetic instability caused by helicase gene mutations will result in increased incidence of cancer (8). When a telomere binder and inhibiter of telomere metabolism, Telomestatin (TMS), was used to study the function of FANCJ helicase in G-quadruplex DNA unwinding of telomeres, DNA damage followed by apoptosis was observed (7). The same study concluded that the presence of G-quadruplex DNA structure within telomeres can also impede DNA replication (7). There is a wealth of data and information recorded to date that argues the need for further investigation to better understand the cellular function, biological importance, and interactions of G-quadruplex DNA structures, especially in relation to DNA helicase proteins (7, 8, 9). By utilizing G-quadruplex DNA-interactive agents, one could potentially alter and change the stability and function of this unusual DNA structure and consequently regulate the behavior of DNA-associated proteins in the form of therapeutic drugs (9, 20).

Thus far, some of the characteristics of the SV40 genome, the function of SV40 T-ag helicase within the viral versus the host cell, and the importance of helicase proteins in proper functioning of cellular processes have been described. Next, the properties and importance of G-rich sequence repeats within the eukaryotic genome and how the quadruplex structure plays a role in cellular functions and genomic stability will be considered.

G-quadruplex DNA structure

There are short DNA sequence repeats of 3-8 guanine residues in length found in different chromosomal sites of eukaryotic genomes, such as telomeres, immunoglobulin switch regions, and promoters (7, 10, 21, 22). Based on bioinformatics studies, the human genome contains up to 376,000 potential sites for G-quadruplex DNA formation (11). The presence of a G-quadruplex DNA complex may contribute to immunoglobulin rearrangement, promoter activation, and telomere maintenance (22, 7). Indeed further research is required to understand the role and biological significance of such G-rich DNA structures within the genome considering that some of these regions are within the telomeric sequence or are highly conserved within the vertebrate genome, such as in CpG islands (11). On the other hand, G-quadruplex DNA formation may cause genomic instability by forming inside the replication fork and stalling the progress of DNA replication (7).

The structure of G-quadruplex DNA can result in various DNA topologies (12, 23). Due to various folding patterns of guanine-rich strands, (e.g. parallel versus anti-parallel) (23, 24), quadruplex DNA can form inter- or intra-molecular (6, 12), unimolecular, bimolecular, or tetramolecular structures (6, 22, 23). In all of these structures, the unusual DNA structure is stabilized via interactions between the guanine residues, which form a planar and symmetrical tetrad ring capable of metal chelation (10, 21, 25). NMR studies of SV40 have shown that a G-rich sequence regions (1,13) containing repeat sequences such as d-TGGGCGGT, which can form a G-quadruplex DNA structure (13). This SV40 G-

rich repeat sequence is considered to be biologically important because of its role in viral encapsidation and that it is a common sequence in CpG islands of the vertebrate genome (13).

The discovery that G-quadruplex DNA-specific proteins play a role within genetic disorders, such as Bloom's (7, 8, 11, 19) and Werner's syndrome (8, 9, 19) has fueled interest in studying G-quadruplex DNA (11). Studies of the human *c-kit* oncogene promoter region (12) and human telomere sequences have shown that G-quadruplex DNA structure can be formed via different pathways (18, 23, 24), found in different structural topologies (12), and within various genome locations (11). The single- stranded G-rich sequence of telomeres at the 3′ end of DNA can fold its four TTAGGG repeats into a unimolecular G-quadruplex structure (18, 21), which may function in protecting the ends of chromosomes from end-to-end fusion (26), prevention of further telomere addition via telomerase activity (18, 21), and base-pair loss (26). The G-rich Telomere DNA sequence at the end of chromosomes shortens with each round of DNA replication referred to as the end replication problem (18). However, a reverse transcriptase protein, telomerase, is able to add G-rich sequence repeats to the telomere strand and render the cell immortal. In fact, more than 85% of tumors exhibit telomerase activity (18).

Inhibition of helicase activity with DNA interactive agents

G-quadruplex DNA formation within promoter regions of certain genes, such as *c-kit*, has emerged as a potential target for anticancer drug therapy (9,

12, 20, 22, 27). Another application of DNA interactive agents is that one can design biological probes for *in vivo* detection of G-quadruplex DNA (21, 25). For the purposes of my research project, the SV40 T-ag helicase which recognizes and unwinds G-quadruplex DNA (10, 15), such as the OR of the SV40 genome, was used to better understand G-quadruplex DNA-helicase interactions. The G4 DNA-helicase interaction was to be examined for its activity and loss of helicase function in the presence of DNA interactive agents.

Studies targeting inhibition of telomerase have shown that G-quadruplex structure negatively regulates telomerase activity by interfering with telomerase loading onto the telomere sequence (21, 26, 28). Similar studies have been conducted for inhibition of helicase enzymes, such as yeast Sgsl helicase (21). The ability of telomere sequences to form G-quadruplex DNA complexes has fueled the idea that one can treat serious diseases by binding of G-quadruplex specific and low molecular weight DNA ligands (9, 29), such as DNA binding of NMM porphyrin which inhibits BLM helicase (9). When designing and studying inhibitory ligands, one has to bear in mind the ability of the ligand to permeate a living cell (27), the possibility of non-specific cellular toxicity caused by same measure of selectivity for duplex versus quadruplex DNA (21), and the affinity or specificity of the ligand compared to naturally occurring DNA binding proteins (27).

The DNA interactive agents addressed and studied in my research consisted of Distamycin A, meso-5, 10, 15, 20-Tetrakis(4-*N*-methylpyridyl)porphine (TMPyP4), CS-86, CS-87, Dictyodendrin B, and Tel 11.

The G-quadruplex DNA binding of these compounds to an intramolecular G-quadruplex DNA substrate was first analyzed and then measured in relation to inhibition of T-ag quadruplex DNA helicase activity. While the basic inhibition approach for T-ag helicase *via* DNA interactive agents is similar to the model shown in Figure 1, the experimental techniques applied were different (4, 30).

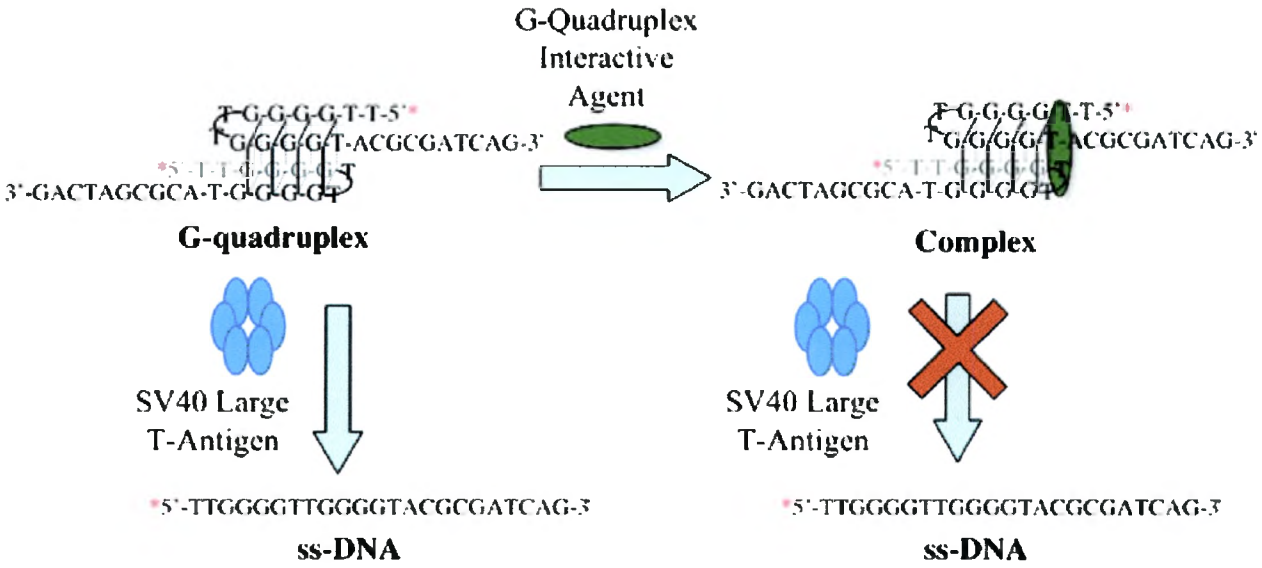

Figure 1. Inhibition of SV40 T-ag G-quadruplex DNA helicase activity by a G-quadruplex binding agent. Certain G-quadruplex DNA interactive molecules confer higher DNA structural stability and inhibit the unwinding of G-quadruplex DNA by T-ag DNA helicase activity (scheme from reference 3).

G-quadruplex DNA interactive agents are often organic, polycyclic, aromatic compounds with a large π-surface (21, 31). Generally, the DNA interactive agents possess a positive charge near the center of the molecule or the side arms, which can increase affinity for the grooves of G-quadruplex DNA

(31). There are various routes for DNA-ligand interaction, such as intercalation between DNA tetrads, end capping or face binding of DNA tetrads, and edge or external binding along DNA tetrad bases (32).

Distamycin A (Figure 2) is an antibiotic (33) that has been previously used as a biological probe in terms of protein interaction with duplex DNA (25). This DNA interactive agent exhibits a different mode of DNA association in the presence of duplex versus quadruplex DNA (25, 34), which offers differential DNA specificity and affinity. NMR studies have shown that Distamycin rings stack on the terminal G-planes of G-quadruplex DNA and intercalate between the G-planes and the bases flanking the G-quartet structure while groove binding is the primary mode of interaction between Distamycin and B-form duplex DNA (25, 33). Since previous studies had reported Distamycin as a specific inhibitor of duplex unwinding by BLM helicase (25), my goal was to closely examine the inhibition of G-quadruplex unwinding by T-ag DNA helicase.

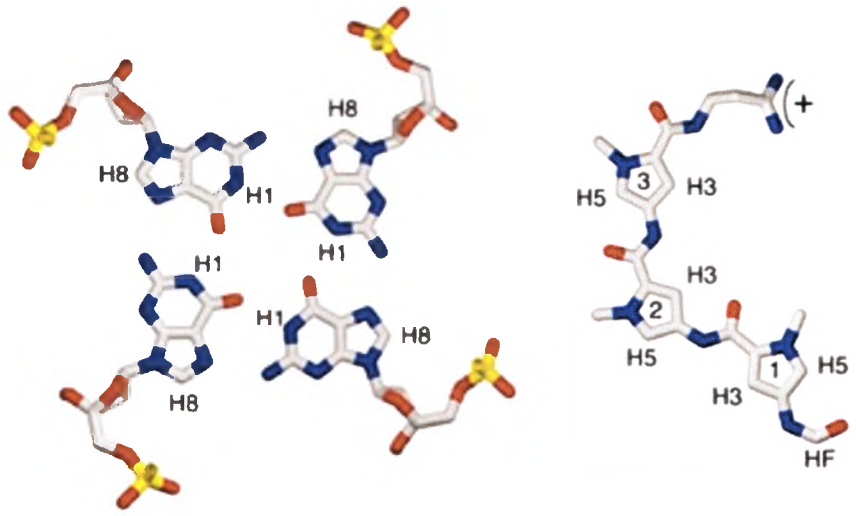

(A) (B)

Figure 2. Structure of G-quadruplex DNA and Distamycin A. The Distamycin rings (B) lie flat on the terminal G-planes of G-quadruplex DNA (A) and intercalate between the G-planes and the bases which flank the G-quartet structure (Figure from reference 25).

Porphyrin molecules, especially water soluble ones, have been extensively investigated in the field of cancer chemotherapy because of their ability to accumulate in cancer tissues while rapidly being metabolized in normal cells (35, 36). TMPyP4 is a cationic porphyrin that has been extensively studied for its strong π–π stacking and electrostatic interaction with G-quadruplex DNA (36, 37). Since the molecular dimensions of this planar porphyrin match well with G-quadruplex DNA (36), TMPyP4 is able to confer further stability on G-quadruplex DNA structures (32, 35, 37), such as that found at human telomere sequences (35). Recent *in vivo* studies have shown tumor reduction in a mouse model by TMPyP4 treatment, presumably through inhibition of telomerase activity (35). Due to the information available about TMPyP4 characteristics, it was

decided to utilize TMPyP4 inhibition as a positive control for inhibition of T-ag G-quadruplex helicase activity

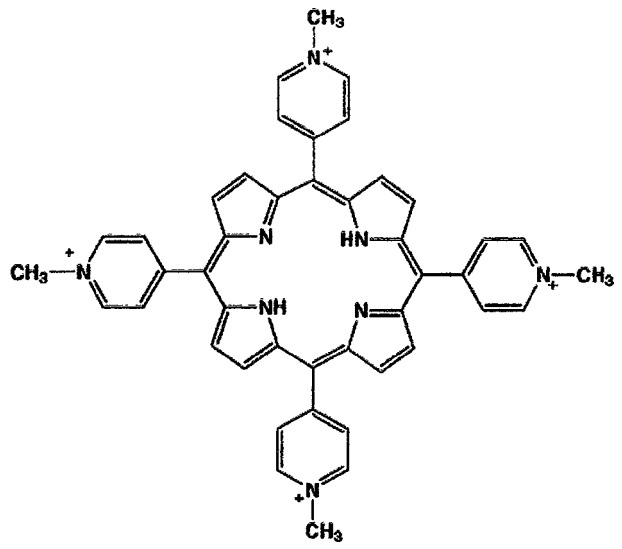

TMPyP4

Figure 3. Structure of TMPyP4. The π–π stacking between the planar core of TMPyP4 and G-tetrads, as well as electrostatic interactions between positively charged constituents of TMPyP4 and the phosphate DNA backbone, allow for a high affinity and strength of G-quadruplex DNA binding (Figure from reference 35).

As a tyramine-based pyrrolocarbazole derivative, Dictyodendrin alkaloid was the first marine natural product that was studied as an antitumor agent for inhibition of telomerase activity (38, 39). It was successfully extracted by reverse-phase HPLC from the marine sponge, *Dictyodendrilla verongiformis*, and the fractions were purified into Dictyodendrin A → E (38). Dictyodendrin has shown complete inhibition of telomerase activity at 50 µg/mL (39). The decarboxylated form of Dictyodendrin A, Dictyodendrin B (Figure 4), was the isolate used in my research project for inhibition of T-ag helicase activity (38).

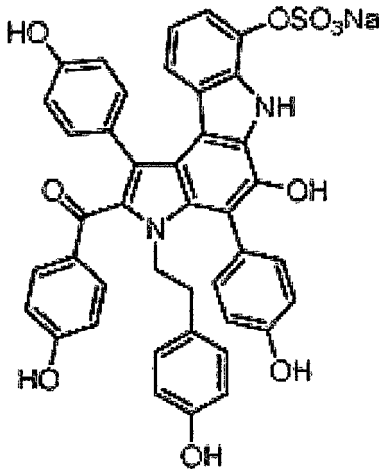

Figure 4. Structure of Dictyodendrin B. Due to the ability to inhibit telomerase activity, Dictyodendrin B was used as a DNA interactive agent in the current T-ag helicase inhibition study. Dictyodendrin B is a tyramine-based pyrrolocarbazole derivative with four *p*-hydroxyphenyl substituents (Figure from reference 37).

Two dihydropyridine derivatives of 3'-azido-2',3'-dideoxyuridine, CS-86 and CS-87, were used in my thesis project (40). In past studies 2, 3 – dideoxynucleosides have exhibited potent inhibition of HIV-1 replication (41) and have been extensively studied as anti-HIV nucleoside drugs that could penetrate the blood brain barrier and suppress viral replication in the brains of AIDS patients (40, 41). As seen in Figure 5 (41), the nucleoside structure of CS-87 showed potential for interaction with G-quadruplex DNA and consequent inhibition of T-ag helicase activity.

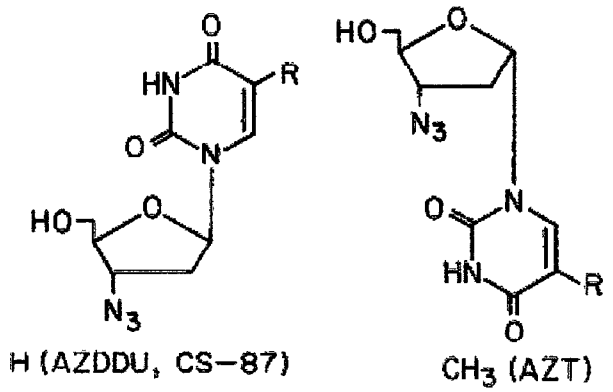

Figure 5. Structure of Anti-HIV drugs, CS-87 and AZT. The nucleoside was designed in an effort to penetrate the blood brain barrier and inhibit DNA replication of the AIDS virus in the brain by viral DNA interaction (Figure from reference 40).

Tel11 (*N,N'*-bis-[3-(4-methyl-morpholin-4-yl)-propyl]-3,4,9,10-perylenetetracarboxylic acid diimide) is a member of the perylene diimides (PDIs) (Figure 6) that have been studied as G-quadruplex-interactive agents and inhibitors of DNA helicase activity (3, 42). The mode of interaction between Tel11 and G-quadruplex DNA is thought to be *via* base stacking on the face of the terminal G-tetrads, which further stabilizes the G-quadruplex structure (3). Previous studies of duplex DNA binding of Tel11 showed inhibition of T-ag DNA helicase activity on duplex DNA (4). Other studies have shown selective binding of Tel11 to G-quadruplex DNA over duplex DNA, especially under conditions favoring aggregation of the ligand (3). Thus Tel11 was a good candidate to study in relation to G-quadruplex DNA binding and inhibition of T-ag DNA helicase activity.

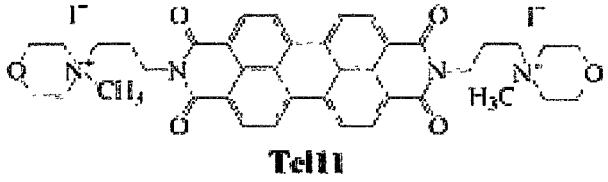

Figure 6. Chemical structure of a perylene diimide (PDI), Tel11. As a water soluble cationic ligand, Tel11 exhibits a higher level of selectivity for G-quadruplex DNA than duplex DNA structure (Figure from reference 42).

Research Strategy and Approach

In order to study DNA helicase activity, it is common practice to use polyacrylamide gel electrophoresis (PAGE) to observe the unwinding of radiolabeled DNA substrates. While the above method works in analyzing the unwinding of duplex or intermolecular quadruplex DNA structures, it is not useful for accurately observing the unwinding of unimolecular G-quadruplex topologies even under native PAGE conditions. Another caveat of using standard SDS-PAGE is the difficulty in observing the mode of inhibition of DNA helicase activity by DNA interactive agents. Consequently, we used a technique in which the DNA helicase activity of a unimolecular G-quadruplex DNA could be better observed.

Among the current technologies available for analysis of biomolecular interactions (43, 44, 45) and measuring the degree of binding affinity (44), Biosensor technologies have become one of the most reliable methods of choice (43). To better observe and describe the type or extent of interaction between SV40 T-ag and G-quadruplex DNA in the presence of DNA-interactive ligands, we used Surface Plasmon Resonance (SPR) (45).

By using the SPR method, which was first described in 1988, one can avoid many of the problems encountered when using alternative techniques, such as microarray analysis that requires labeling (43, 44) or stop flow technologies that are time- and material-consuming (43). On the other hand, SPR is performed in real time (43) and is a label-less method (10, 43). Conventional methods such as NMR or X-ray crystallography provide detailed structural information while calorimetric studies provide thermodynamic information of DNA-ligand interactions but all are in the realm of steady state kinetics with little to no dynamic information, such as association and dissociation rate constants between DNA and ligand (29) SPR technology is based on optical detection principles (43, 44) where factors governing the data obtained from SPR are based on binding affinity, density of biomolecules bound to the chip, flow cell concentration, and the kinetic rate of molecular interactions (45) The SPR sensor chip needs to be composed of a material with efficient electric conductivity, such as copper (Cu) or gold (Au) (43). The kind of sensor chip used for my research project was a gold chip coated with streptavidin (SA), referred to as a SA sensor chip The strong biotin-streptavidin interaction was used to immobilize biotinylated ligand (DNA substrates) onto the SA sensor chip

The sensorgram graph and data generated by SPR is reported in terms of Response Units (RU) (45), which exhibits a relationship between a change in reflected light intensity and mass of the biomolecules bound to the chip (44). Therefore, molecular mass changes are calculated via changes in the intensity of reflected light (44).

The strategy of my project was to immobilize unimolecular G-quadruplex DNA substrates onto SPR (SA) sensor chips followed by injection of various types of small inhibitory DNA interactive compounds (Figure 7). This was followed by injection of T-ag helicase, which allowed for real time observation of DNA binding and unwinding events. Due to the properties of SPR technology, association and binding of molecules to the immobilized DNA would lead to an increase in the RUs observed on the sensorgram. On the other hand, removal of molecules or DNA from the SA sensor chip would lead to a decrease in the RUs observed, which corresponds to the amount of mass removed.

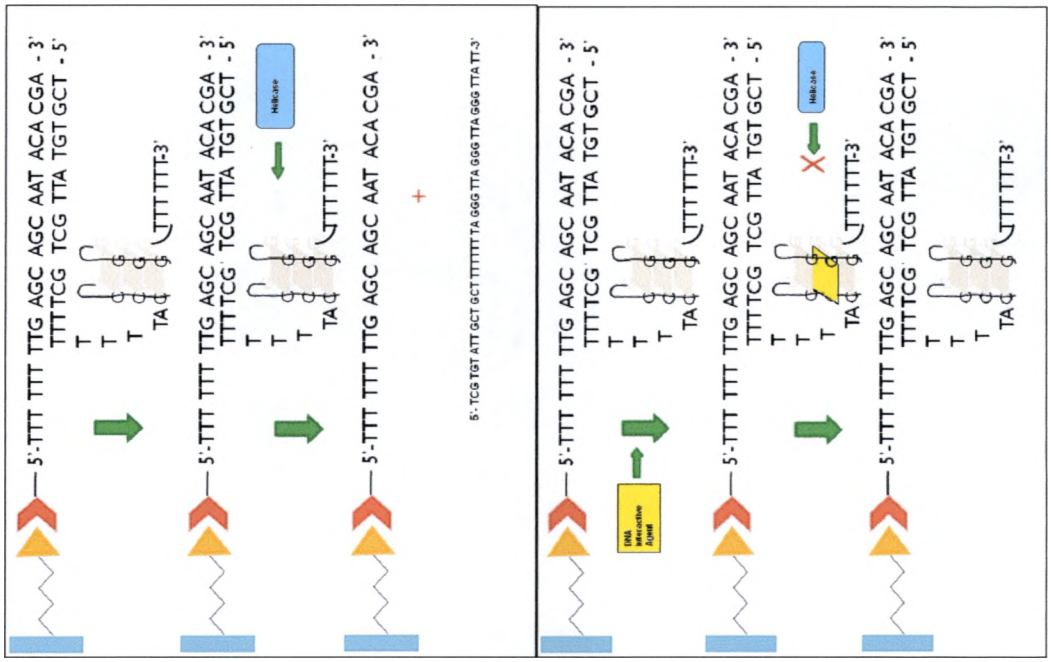

Figure 7. Strategy for observing T-ag G-quadruplex helicase activity and inhibition. In the presence of a G-quadruplex DNA interactive agent, T-ag helicase activity is inhibited (right). In the absence of a DNA interactive agent, T-ag helicase binds and unwinds G-quadruplex DNA, leaving the biotinylated DNA behind (left).

Previous study has shown the ability of T-ag to unwind intramolecular quadruplex 5'-(TTT GGG)$_4$ TT-3', as observed by SPR (4). For the purposes of my project, several different DNA substrates were used, one of which is shown in Figure 7. The complementary oligonucleotide (to the immobilized strand) contained a G-rich region at the 3'-end capable of unimolecular quadruplex formation. The complementary DNA strand also had a 3'-overhang where T-ag was forced to bind and unwind the quadruplex structure prior to unwinding the duplex region. In another series of similar experiments, the biotinylated DNA substrate was composed of a unimolecular quadruplex forming region near the 3'-end while the 5'-end was biotinylated. In this case, the complementary DNA strand was designed to have a 3'-overhang and form a short duplex DNA structure. The T-ag would be forced to bind and unwind the immobilized quadruplex DNA prior to unwinding the short duplex structure. Upon complete unwinding of either substrate *via* T-ag helicase activity, the complementary DNA strand would be removed from the SA sensor chip along with a decrease in the observed RUs. The small inhibitory DNA molecules were aimed at associating with the quadruplex forming region of the DNA substrate. In a successful inhibition of T-ag helicase activity, the helicase would be unable to unwind the quadruplex region of the DNA, and the decrease in RUs would not occur to the extent expected.

CHAPTER II

MATERIALS AND METHODS

1 Chemicals and Reagents

Reagents used for the preparation of buffer solutions were purchased from Sigma-Aldrich (St. Louis, MO) or GE Healthcare (Piscataway, NJ), unless otherwise noted. Potassium Chloride and Magnesium Chloride were purchased from EM Science (Gibbstown, NJ). The following buffers: KCl HBS-EP buffer (0 01 HEPES, pH 7.4, 0.15 M KCl, 3 mM EDTA, and 0.005% v/v P20 surfactant), MgCl/KCl HBS-EP buffer (0.01 HEPES, pH 7.4, 0.15 M KCl, 3 mM EDTA, 10 mM $MgCl_2$ and 0.005% v/v P20 surfactant), NaCl HBS-EP buffer (0.01 HEPES, pH 7.4, 0.15 M NaCl, 3 mM EDTA, and 0 005% v/v P20 surfactant), and NaCl/MgCl buffer (0.01 HEPES, pH 7.4, 0.15 M NaCl, 3 mM EDTA, 10 mM $MgCl_2$ and 0.005% v/v P20 surfactant) were utilized as working stock buffer solution. Any modifications made to the content or the concentration of the stock buffers mentioned above, for experimental purposes, are noted in the individual methods. It was standard procedure to degas and filter all of the buffers with 0.2 µm filters (Nalgene) prior to each use. Upon filtration, the degassing was

accomplished by leaving the buffer under vacuum suction for at least 10 minutes The goal was to have little to no air bubbles present within the buffer. The DNA sequences were purchased from Integrated DNA Technologies (Coralville, IA). The biotin-labeled DNA sequences were HPLC purified; other DNA sequences were PAGE purified or desalted without further purification. The DNA sequences shown in Table 1 were used for this thesis project.

SV40 T-ag helicase was supplied by CHIMERx. CHIMERx isolated SV40 T-ag from cultured insect cells and stored it in 10 mM Tris-HCl, pH 8.0, 100 mM NaCl, 1.0 mM EDTA, 1.0 mM dithiothreitol, and 50% (v/v) glycerol. The SV40 T-ag (aliquote 1.9 µg/µL) was used with no further purification procedures The aliquots of SV40 T-ag were stored at -80°C Prior to use, each enzyme aliquot was diluted to the desired concentration within MgCl HBS-EP buffer.

For the T-ag helicase inhibition studies, TMPyP4 [5, 10, 15, 20-tetrakis (*N*-methyl-4-pyridyl) porphine] and Distamycin A were purchased from Sigma-Aldrich while CS-86, CS-87, Tel 11, and Dictyodendrin B were provided as a gift from Dr. Sean Kerwin's lab at The University of Texas at Austin (Austin, TX).

The BiacoreX instrument was used for experiments involving Surface Plasmon Resonance (SPR). The SPR sensor chip obtained from GE healthcare was derivatized with streptavidin, called a SA chip. The SPR is designed to measure the change in refractive index on the gold (Au) surface of the sensor chip, referred to as response unit (RU). Once a biotinylated ligand (L) is immobilized on the SA chip, an analyte (A) is introduced. The binding of the analyte to the ligand causes a change in the refractive index, which consequently

changes the RU detected and observed on the sensorgram One RU is representative of 1 pg of mass on the surface of the sensor chip (4).

Table 1. Summary of DNA Sequences. The sequences which contain a 5′-BioTEG linker were immobilized as ligands on the SPR SA sensor chip.

DNA	*Sequences*
TAG DNA1	5′-BioTEG-TTTTTTTTGAGCAGCAATACACGA-3′
TAG DNA2	3′-CTCTCTCTCTCTCGTCGTTATGTGCT-5′
TAGcompG4	3′-TTTT(GGGATT)$_4$CCCGTTATGTGCT-5′
ImG4	5′- Bio TEG-TC GTG TAT TGC TGC TTT TTT (TTAGGG)$_4$ TT- 3′
ImG4comp1	3′- CAC ATA ACG ACG A- 5′
ImG4comp2	3′- CAC ATA ACG ATT T- 5′
G4duplexTEST	5′- ATCCCAATCCCAATCCCAAT-3′

2. Previous Experiments

Recent studies conducted in Dr. David's lab were mainly aimed at characterizing and identifying optimal conditions of important factors, such as ATP nucleotide concentration, KCl and/or MgCl HBS-EP buffer concentration, and T-ag helicase concentration. The optimal parameters were to be followed for future studies of T-ag DNA helicase activity as well as G4-quadruplex structure formation of the G-rich human telomere sequence. The optimal SPR assay conditions were determined by previous studies (4, 30) to be the following: 150 mM KCl HBS-EP, 150 mM NaCl HBS-EP, 10 mM MgCl HBS-EP, 40 mM ATP, and 2.9 nM SV40 T-ag helicase (hexamer concentration). These conditions were held constant, unless otherwise noted.

The main goal of my research project was to pursue investigation of inhibition studies involving unimolecular G4-quadruplex DNA containing the

human telomere sequence. Some of the inhibitory compounds used were the same as those used in previous T-ag inhibition studies for duplex DNA (4, 30) while others (e.g. Dictyodendrin B) had not been previously investigated in a T-ag DNA helicase inhibition study.

3. Preparation of duplex DNA substrates

The formation of duplex DNA on the Streptavidin (SA) sensor chip was accomplished by immobilization of biotinylated single-stranded DNA, called TAG DNA1. The complementary DNA strand, TAG DNA2, was then diluted in HBS-EP buffer to a concentration of a 100 μM. The complementary DNA strand was then injected in 50 μL increments over the flow cell surface at a flow rate of 5 μL/min. The injected complementary DNA strand would interact and bind to the immobilized biotin-containing DNA via base-pairing. The small injections would continue until the flow cell of the sensor chip appeared to be fully hybridized and we could not observe a further increase in the RU of the sensorgram. The change in RU exhibiting maximum hybridization was calculated via the following equation:

(Eq. 1) $$R_{max} = RU_{im} * (MW_A / MW_L) * S$$

The R_{max} refers to the response representing 100% hybridization, RU_{im} is the increase in RU that is observed upon immobilization of the biotinylated DNA strand onto the sensor chip, MW_A is the molecular weight of the complementary

DNA strand (analyte), and MW_L is the molecular weight of the immobilized biotinylated single stranded DNA. The interaction taking place between the two DNA strands is at a ratio of 1:1 binding interaction. Thus the multiplication of value of the above R_{max} by binding stoichiometry factor (S) is not needed.

4. Preparation of G-quadruplex substrates

The binding of a single strand of DNA on a Streptavidin (SA) sensor chip was accomplished by immobilization of a biotinylated single strand of DNA (TAG DNA1). The complementary quadruplex forming DNA strand, TAGcompG4, was diluted in HBS-EP buffer to a concentration of a 100 µM. TAGcompG4 was designed to form fourteen base-pairs with TAG DNA1 strand followed by a poly T spacer. On the other side of the poly T spacer was the human telomeric sequence $(TTAGGG)_4$ followed by a longer poly T 3' tail. The complementary DNA strand was injected in 50 µL increments over the flow cells at a flow rate of 5 µL/min The complementary portion of the quadruplex DNA strand would interact and bind to the immobilized biotin bound DNA via base-pairing. The G-rich region near the 3' overhang of TAGcompG4 that was not complementary to the immobilized DNA would fold into a unimolecular quadruplex DNA structure. The small 5 µL injections of complementary DNA strand continued until the targeted flow cell of the sensor chip appeared to be mostly hybridized (800 – 1000 RU). The change in RU exhibiting maximum hybridization of DNA was calculated from Eq. 1.

Later in the inhibition studies, another strand of G-quadruplex forming DNA was designed that was itself biotinylated so that it could be immobilized on the SA sensor chip, called ImG4 DNA. Complementary DNA strand studies showed that the best candidate strand was one that contained an overhang tail at its 5'-end (G4comp2) compared to a complementary DNA strand with blunt ends (G4comp1).

The same immobilization and hybridization protocol was followed for ImG4 and its complementary strand as was previously mentioned for the TAGcompG4 DNA, unless otherwise noted. The change in RU exhibiting maximum hybridization was calculated from the same equation as for duplex DNA (Eq. 1)

5. DNA binding assay of inhibitory compounds

5.1 DNA binding assay of CS-86 and CS-87 to double-stranded DNA.

Both CS-86 and CS-87 were related synthetic compounds that due to their properties and structure were considered each to be a candidate for duplex or G-quadruplex DNA binding and potential inhibition of DNA unwinding by T-ag helicase. Prior to performing an inhibition study, a DNA binding assay was necessary to evaluate the binding specificity of inhibitory compounds to duplex versus quadruplex DNA, specifically where there were no prior DNA binding data available. To do a duplex DNA binding assay, serial dilution of the DNA interactive ligand were made in 150 mM NaCl/MgCl HBS-EP buffer. The concentration of CS-86 (98 μM) and CS-87 (98 μM) was each made in the following order: 250 nM, 500 nM, 1 μM, and 2 μM.

Upon full hybridization of DNA onto immobilized DNA at a rate of 20 µL/min, 80 µL of the potential T-ag inhibitory compound was injected onto the flow cells at the same flow rate as the DNA hybridization injections. Upon completion of the injection, the baseline of the sensorgram was allowed to stabilize for approximately 10 min. For washing of the flow cells from any remaining bound compounds, 10 µL of Karl's regeneration buffer (2 M - guanidine HCl, 10% (v/v) formamide, and 0.1% surfactant P20) was injected over the flow cells at 20 µL/min flow rate. The regeneration injections were performed two to three times at the end of each experiment to regenerate the SA chip. The experiments were repeated in triplicate.

Based on the results, it was decided to dismiss CS-86 and CS-87 from future inhibition studies. Instead, it was decided to perform T-ag helicase inhibition studies with other synthetic compounds, such as Tel 11, which had been previously shown to inhibit T-ag helicase activity when bound to duplex DNA.

5.2 DNA binding assay of Tel 11 to double-stranded DNA.

Serial dilution of Tel 11 (200 µM) was made with 150 mM NaCl/MgCl HBS-EP buffer at concentrations of 250 nM, 500 nM, 1 µM, and 2 µM. The protocol described for CS-86 and CS-87 was followed for the DNA binding assay of Tel 11. The experiment was only conducted once due to solubility issues

5.3 DNA binding assay of Dictyodendrin B to G-quadruplex DNA.

Up to this point of T-ag inhibition studies, the selected inhibitory molecules were synthetic compounds. Recent studies involving a natural compound, Dictyodendrin B, had shown inhibitory effects on the enzymatic activity of DNA telomerase (39). These findings encouraged our lab to obtain the compound and conduct inhibition studies with T-ag DNA helicase instead of DNA telomerase. Due to the fact that there was no previous study conducted about Dictyodendrin B inhibition of T-ag DNA helicase activity, a DNA binding assay was performed to decide the DNA binding specificity of this compound at different concentrations for duplex versus G-quadruplex forming DNA strands. Dictyodendrin B (180 μM) was serially diluted in 150 mM KCl/MgCl HBS-EP buffer to yield concentrations of 500 nM, 1 μM, 2 μM, 4 μM, and 8 μM. The DNA binding assay examined and compared the association and dissociation of the compound from the DNA at different concentrations. The protocol described previously for duplex DNA binding assay was followed for G-quadruplex DNA binding assay of Dictyodendrin B.

To reduce the chance of any non-specific binding or interaction, the SA sensor chips were no longer fully hybridized. Instead, only 200 to 400 RU's of the complementary strand was hybridized onto the SA chip. Experiments were performed in duplicate.

6. Inhibition of T-ag G-quadruplex DNA helicase activity

6.1 Inhibition of T-ag helicase activity via G-quadruplex DNA binding of Tel 11.

Serial dilution of Tel 11 (200 μM) was performed with 150 mM KCl/MgCl HBS-EP buffer yielding the following concentrations: 250 nM, 500 nM, 1 μM, 2 μM, 4 μM, and 6 μM. The T-ag was diluted in 150 mM KCl/MgCl HBS-EP buffer. The ATP nucleotide was dissolved separately in 150 mM KCl/MgCl HBS-EP buffer. Right before injection, the T-ag and ATP were combined at a 1:1 ratio. The regeneration solution used consisted of 1M KCl and 50 mM NaOH buffer. Experiments were conducted under optimal conditions with a flow rate of 5 μL/min. After DNA hybridization, the injection of inhibitory molecules over the flow cells was performed under "manual injection" mode. By doing so, the operator could stop and restart the injection at any time during the manual injection. This feature was important and used for injecting the T-ag helicase enzyme. Once the sensor chip was fully hybridized at about 800 to 1000 RU's with complementary DNA strand (TAGcompG4), 50 μL of Tel 11 was injected at 5 μL/min onto the flow cells while under manual injection mode. Once the injection module showed a total injection volume of 50 μL, the flow was temporarily stopped. 60 μL of ATP and T-ag combined mixture was injected and the flow was manually restarted. Once the desired injection volume of T-ag was reached, the flow was stopped and the manual mode was exited which allowed for normal flow to resume. The baseline of the sensorgram was allowed to stabilize for five to ten minutes. To regenerate the flow cells, the flow rate was increased from 5 μL/min to 30

µL/min. To remove any remaining Tel 11, 10 µL of 1 M KCl/ 50 mM NaOH regeneration buffer was injected for two to three times. The experiment was repeated in duplicate. The percent unwound DNA for each inhibitor molecule concentration after the end of T-ag injection was calculated. To calculate the % unwound DNA the following formulas were used with the example given from calculations used to generate Table 2

(Eq. 1) $R_{max} = RU_{im} * (MW_A / MW_L) * S$

(Eq. 2) RU difference = RU final - RU initial

(Eq. 3) % Unwound = (RU difference / R_{max}) * 100%

Example:

R_{max} = 958 RUs x (0.45) (1:1)

R_{max} = 431.5 RUs

RU difference = 24871.1 RUs - 2141.3 RUs

RU difference = 345.8 RUs

% Unwound = 345 RUs/ 431.5 RUs

% Unwound = 80% of DNA was unfolded

6.2 Inhibition of T-ag DNA helicase activity by G-quadruplex DNA binding of TMPyP4.

The compound chosen for the following inhibition study was one of the compounds used by the lab in a previous inhibition study involving duplex DNA (4). The results from the previous study showed that TMPyP4 did indeed hinder

the T-ag DNA helicase activity upon duplex DNA binding. TMPyP4 (200 μM) underwent serial dilution with 150 mM KCl/MgCl HBS-EP buffer yielding the following concentrations: 250 nM, 500 nM, 1 μM, and 2 μM. The conditions in which the experiment was conducted were optimal. The regeneration buffer used for this experiment was 1 M KCl/ 50 mM NaOH buffer. The experiment was performed in duplicate.

6.3 Inhibition of T-ag DNA helicase activity by G-quadruplex binding of Distamycin A.

Distamycin A is an antibiotic that was another candidate for binding to G-quadruplex DNA and potentially inhibiting T-ag DNA helicase activity. The molecule was shown from a past duplex DNA inhibition study to provide inhibition of T-ag helicase activity after binding to duplex DNA. Under optimal conditions, Distamycin A (2 mM) underwent a serial dilution with 150 mM KCl/MgCl HBS-EP buffer yielding the following concentrations: of 250 nM, 500 nM, 1 μM, 2 μM, 4 μM, and 10 μM. The protocol used for this experiment was the same as the protocol described in Tel 11 inhibition study. The % unwound DNA was calculated as previously described (Eq. 1, 2, and 3). The experiment was conducted in duplicate.

Based on the inhibition study results from Distamycin A and Tel 11 involving binding of G-quadruplex DNA, it was necessary to check the potency or quality of the compounds by repeating some of the T-ag duplex DNA helicase inhibition studies performed by our lab previously where some degree of

inhibition of T-ag helicase activity via DNA binding of Distamycin A, Tel 11, and TMPyP4 was observed

A new SA chip was immobilized with TAG DNA1 followed by hybridization with complementary DNA strand TAG DNA2. As described before, the two DNA strands form duplex DNA. The inhibitory compounds, Tel 11 and Distamycin A, were each diluted with 150 mM NaCL/MgCl HBS-EP buffer to a concentration of 1 μM and 4 μM. The results of this experiment concurred with previous results from our lab and verified the quality and degradation level of these two DNA interactive molecules.

6.4 G-quadruplex formation on the 3'-overhang tail of TAGcompG4 DNA in the presence of KCl HBS-EP versus LiCl HBS-EP buffer.

The results obtained so far from the inhibition studies involving Tel 11, TMPyP4, and Distamycin A prompted the design of an experiment to measure the level of G-quadruplex DNA formation in the presence of a strong G-tetrad stabilizing ion, such as potassium versus a weak G-tetrad stabilizing ion, such as lithium (46). To test whether 150 mM KCl HBS-EP buffer was the appropriate ion concentration used for G-quadruplex DNA formation, a serial dilution of KCl in HBS-EP buffer was made in the following order: 15 mM, 50 mM, and 150 mM. 150 mM of LiCl HBS-EP buffer was made to compare our 150 mM KCl HBS-EP buffer to a weak G-tetrad stabilizing ion

Since TAGcompG4 DNA consists of human telomeric G-rich DNA sequence with a 3′-overhang tail, it is supposed to form a stable G-quartet

structure in the presence of potassium, as a strong chelating ion. To measure the percentage or ratio of G-quadruplex DNA formation accurately, a new strand complementary to the TAGcompG4 DNA was designed, called G4duplexTEST. The newly synthesized G4duplexTEST DNA was made to the same concentration as TAGcompG4 DNA. The G4duplexTEST DNA sequence was designed to be complementary to the G-rich 3′-overhang tail of G-quadruplex DNA strand. G4duplexTEST is able to bind to TAGcompG4 DNA strand only when TAGcompG4 is not folded into a G-quadruplex structure (Figure 13). The TAGcompG4 DNA was fully hybridized (~ 1000 RUs) to the immobilized TAG DNA1 strand followed by 20 µL injection of G4duplexTEST strand. The amount of G4duplexTEST strand bound to the immobilized TAG DNA1 strand would correspond to the RU increase on the sensorgram. The percent change in the RU was measured and translated into G4duplexTEST binding to an unfolded human telomere sequence of TAGcompG4 strand. The TAGcompG4 DNA binding of G4duplexTEST was calculated within each of the different concentrations of KCl HBS-EP and LiCl HBS-EP buffers by using equation 1, 2, and 3. In this experiment G4duplexTEST was treated as the analyte and the TAGcompG4 as the ligand. The results obtained from this experiment led to the continued use of 150 mM KCl HBS-EP buffer.

6.5 Efficiency of DNA helicase activity of T-ag in relation to blunt end versus 3´-overhang tail containing DNA strands.

Due to the high efficiency of T-ag DNA unwinding in our studies, the removal of the G-quadruplex DNA strand from the chip even in the presence of 10 μM bound compounds, it was decided to design a different and more stable type of G-quadruplex DNA strand with the same human telomere G-rich sequence.

To ensure that the robust DNA helicase activity and removal of complementary DNA strands from the SA chip was not due to an unstable environment caused by steric effects between the quadruplex structures bound to immobilized DNA *via* 16 base pairs, the new biotinylated immobilized DNA was designed to contain the G-quadruplex forming human telomere sequence near the 3´-overhang. Two types of strands were tested as potential complements for the new immobilized DNA strand, called ImG4. One of the candidate strands had blunt ends, called G4comp1, while the other candidate strand contained an overhang tail at its 5'-end, called G4comp2. The goal of this experiment was to observe the efficiency of DNA unwinding by T-ag when faced with blunt end DNA versus 5´-overhangs. The experiment was done in duplicate.

Based on the results, the ImG4 complementary DNA strand which exhibited efficient T-ag enzymatic activity was selected. The goal was to keep the helicase activity of the T-ag and ensure that any inhibition of the T-ag activity was not due to the structure of the new complementary DNA strand.

Since G4duplexTEST was also complementary to the single stranded 3'-end sequence of ImG4, a similar G-quadruplex formation study was performed to test the percentage of G-quadruplex DNA formation of ImG4 in the presence of 150 mM KCl HBS-EP buffer. Based on the results, G-quadruplex formation in ImG4 was verified and it was decided to use ImG4 for future inhibition studies. The experiment was performed in triplicate.

6.6 Reaching half enzyme activity via manipulation of T-ag helicase and ATP nucleotide concentrations.

The kind of results obtained so far pointed the study towards examining the activity level of the helicase enzyme, SV40 T-ag. The results obtained from T-ag inhibition experiments involving ImG4 DNA was identical to previous results obtained using TAGcompG4. As mentioned before, optimal conditions that were determined by past duplex DNA inhibition study (4, 30) were followed to allow for comparison between our duplex and G-quadruplex T-ag inhibition studies To begin this experiment, the concentration of T-ag enzyme was first reduced from 2.9 nM hexamer to 0.29 nM. Due to no change in helicase activity, the concentration of T-ag was reduced by a 1000 fold to 2.9 pM. To reduce material waste, the injection volume of the T-ag and ATP mixture was reduced from 80 to 40 µL with no change observed on the sensorgram for full T-ag helicase activity at 2.9 pM. Based on a lack of decrease in T-ag helicase activity, it was decided to manipulate the ATP concentration needed for the T-ag helicase activity Instead of using a saturated concentration of 40 mM ATP nucleotide, it was

decided to use the T-ag at 2.9 pM concentration and do a serial dilution of different concentrations of ATP. The concentrations made for the ATP assay were 5 mM, 10 mM, 15 mM, and 40 mM.

Except for a change in concentration of T-ag and ATP molecule, other experimental parameters for buffer and DNA concentration remained the same as mentioned before. In the absence of any DNA interactive compound, 40 µL of T-ag and ATP mixture was injected and introduced at 20 µL/min to the immobilized ImG4 DNA, which was G4comp2 DNA strand hybridized. The degree of the DNA unwinding by T-ag helicase was measured as a change in RU in the presence of each ATP concentration. To regenerate the sensor chip, 30 µL of Karl's regeneration buffer was injected two to three times at 50 µL/min flow rate. The ATP concentration which yielded half T-ag DNA helicase activity was used for future inhibition study. Enzyme activity was calculated as described earlier (Eq. 1, 2, and 3). Experiments were conducted in duplicate.

6.7 Inhibition of T-ag helicase activity by Distamycin A binding to G-quadruplex DNA (ImG4) at half enzyme activity.

For the inhibition studies mentioned hereafter, the enzyme activity was maintained to 50%. This was meant to simulate a more realistic cellular condition in regards to ATP nucleotide availability and enzyme concentration. The first compound chosen here for quadruplex DNA inhibition study was Distamycin A, which was earlier mentioned to inhibit T-ag DNA helicase activity upon binding to duplex DNA (25, 34). A serial dilution of Distamycin A was made with 150 mM

KCl/MgCl HBS-EP buffer in the following order: 4 μM, 8 μM, 10 μM, and 40 μM. The concentration of the 40 μL T-ag and ATP injection used for future inhibition studies contained 2.9 pM and 15 mM, respectively. The experiment was conducted at 20 μL/min flow rate. 30 μL of Karl's regeneration buffer was used for regenerating of the sensor chip at 50 μL/min rate. Other than the modification made to the concentration of ATP and T-ag, the remainder of the protocol was the same as previously described for T-ag inhibition study. The experiment was performed in duplicate. For calculating % unwound, equation 1, 2, and 3 was used

6.8 Inhibition of DNA helicase activity of T-ag by TMPyP4 binding to G-quadruplex DNA at half enzyme activity.

To compare and confirm that the results obtained from Distamycin A inhibition at half enzyme activity was reproducible with other potential inhibitory compounds, TMPyP4 (200 μM) was chosen to be tested as the next T-ag inhibitory molecule. TMPyP4 was made at a concentration of 1 μM and 4 μM via serial dilution with 150 mM KCl/MgCl HBS-EP buffer. The parameters used for this experiment were kept the same as the half enzyme activity experiment involving Distamycin A. The experiment was performed in duplicate.

CHAPTER III

RESULTS AND DISCUSSION

Initially, the main goal of my thesis project was to better understand and observe the interaction between unimolecular G-quadruplex DNA and T-ag DNA helicase using real time SPR. This would be possible by inducing inhibition of T-ag DNA helicase activity via G-quadruplex DNA binding ligand. The T-ag G-quadruplex helicase activity and inhibition by several DNA interactive agents at different concentrations was investigated. As the DNA binding assays and T-ag inhibition studies proceeded, it was apparent that the experimental conditions followed from previous SPR studies for T-ag duplex helicase activity and inhibition (4, 30) were not ideal for the purposes of our study.

Previous T-ag duplex DNA helicase experiment in the David lab, which demonstrated inhibition of T-ag helicase activity in response to DNA binding by Distamycin A and Tel11 were repeated and the potencies of the DNA ligands were confirmed. The formation of quadruplex structures in the immobilized DNA substrates was also confirmed by performing a second G-quadruplex formation experiment at 150 mM KCl. Thus it was then deemed necessary to review and modify the parameters adapted from past SPR-based optimization assays (4,

30). Once the parameters were modified, it was possible to see the effect of some DNA interactive agents on T-ag helicase inhibition when associated with G-quadruplex DNA. A different level of T-ag DNA helicase inhibition was observed at different concentrations of the same compound, which exhibited dose dependence The level of inhibition varied at the same concentrations for different DNA interactive compounds, which suggests that variable DNA binding by different DNA interactive agents resulted in different levels of T-ag DNA helicase activity and inhibition.

1.DNA binding assay of inhibitory compounds

1.1 DNA binding assay of Cs-86 and Cs-87 to double-stranded DNA.

In past studies (40, 41, 46) nucleoside analogues have been extensively studied in the field of anti-HIV therapy. AZT, a dihydropyridine compound, was the first drug treatment available for AIDS patients (41). The potent inhibition of viral replication of human immunodeficiency virus (HIV) in the brain of AIDS patients with such nucleosides fueled interest in examining their inhibition of SV40 T-ag helicase activity (40, 41). Prior to performing a T-ag helicase inhibition study, a DNA binding assay with the two dihydropyridine derivatives (40), CS-86 and CS-87, was performed. For the purposes of future medicinal applications, it is not advantageous to use a DNA interactive molecule which exhibits non-specific DNA binding that is independent of its concentration or DNA structure, such as duplex versus G-quadruplex DNA binding If an inhibitory DNA ligand was to be considered as a therapeutic drug, it is necessary to ensure that it

exhibits higher selectivity and binding affinity for the target DNA, which in this case was unimolecular G-quadruplex DNA (TAGcompG4).

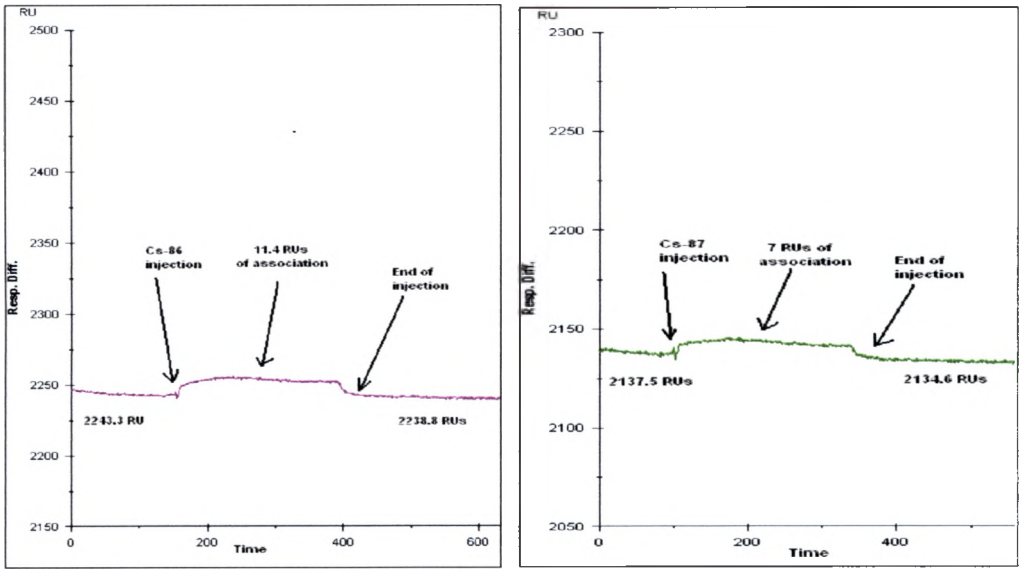

(A) **(B)**

Figure 8. Duplex DNA binding assay of CS-86 and CS-87 molecules. (A) 1 μM of CS-86 was introduced to immobilized duplex DNA. Upon the completion of CS-86 injection, the RU dropped to its initial level. (B) 1 μM of CS-87 is introduced to immobilized duplex DNA. In both cases, CS-86 and CS-87 is washed out of the flow cell and does not exhibit high affinity or specificity to duplex DNA. The amount of TAG DNA1 immobilized was ~ 800 RUs. It was fully hybridized by TAG DNA2. The sensorgram trace is reference subtracted to account for non-specific binding and bulk buffer effects. The sensorgram has an "injection start" and "end of injection" spike due to slight time delay between injection through flow cell 1 and 2.

Upon conducting the duplex DNA binding assay of CS-86 and CS-87 at concentrations ranging from 250 nM to 2 μM, it was apparent from the SPR sensorgrams that both these candidate G-quadruplex DNA interactive agents exhibited no association with duplex DNA. There was no specificity observed at different concentrations of CS86 or CS87 for duplex DNA binding. As seen in Figure 8, the RU drops back to its initial RU of hybridized DNA as soon as the

injection of CS-86 or CS-87 is complete and followed by a wash The same pattern of dissociation shown in Figure 8 was observed at different concentrations of CS-86 and CS-87 (data not shown). A DNA binding study of CS-86 and CS-87 was performed by another member of the David lab using electrospray ionization mass spectrometry (ESI-MS) instead of SPR The study yielded a pattern of no association with DNA (data not shown) Based on the DNA binding assay results and the MS results obtained, it was decided not to further pursue T-ag G-quadruplex helicase inhibition study using CS-86 or CS-87 In the case of a nucleoside such as CS-86 or CS-87, the compound could be experiencing weak interactions binding to the duplex DNA due to the size and structure of the compounds. Even though both CS-86 and CS-87 are planar and polar (41), the binding in this study was negligible.

1.2 Duplex DNA binding assay of Tel11.

Tel11 is a PDI molecule tested in previous studies (3, 21, 30, 42, 47) and shown by a previous SPR-based inhibition study (3, 30) to inhibit T-ag DNA helicase activity on duplex DNA. An ESI-MS study for DNA binding of various PDI molecules revealed a high level of specificity of Tel11 for binding of G-quadruplex DNA, although it can also associate with duplex DNA (48) This finding can be used to explain the results obtained from a previous SPR-based inhibition study of T-ag helicase activity via duplex DNA binding of Tel11 (30). It was necessary to study Tel11's binding to G-quadruplex DNA and potential inhibition of T-ag DNA helicase activity. Before doing so, the plan was to conduct

a duplex DNA binding assay of Tel11 at concentrations ranging from 250 nM to 2 μM. This experiment had to be terminated abruptly after clogging of the SPR flow cells began to occur frequently, especially after each injection of Tel11 into the flow cells. It was concluded at that time that Tel11 was not an appropriate candidate to be used on the SPR instrument at concentrations higher than 2 μM, especially since the flow cells of the Biacore were being used frequently and on daily basis. The challenge with studying some of the potential T-ag inhibitory molecules is that they may cause blockage of the flow cells by precipitating out of solution and clogging the flow of material throughout the instrument. This is why performing routine weekly maintenance and applying regeneration buffer after each experiment to wash the flow cells and remove any remaining molecules was very important. While lacking the complete picture of Tel11 binding to G-quadruplex DNA using SPR, study of Tel11 inhibition of T-ag helicase activity was resumed after the purchase of a new flow cell, which was less prone to clogging.

1.3 Binding of Dictyodendrin B to G-quadruplex DNA.

Inhibition studies of telomerase activity have shown Dictyodendrin alkaloids (A—E) to be potent inhibitors of telomerase activity (38, 39). Due to the inhibitory effects of Dictyodendrin alkaloids on telomerase activity, it was decided to study the inhibition by a naturally occurring Dictyodendrin alkaloid, Dictyodendrin B (38). Before doing so, a study of the binding of Dictyodendrin B to G-quadruplex DNA (ImG4) was conducted. As can be seen in Figure 9, the

alkaloid was injected at concentrations ranging from 500 nM to 8 μM with no dose dependent specific binding observed. In fact, upon the end of each Dictyodendrin B injection into the flow cells, the RU stabilized back to the same RU level of hybridized DNA.

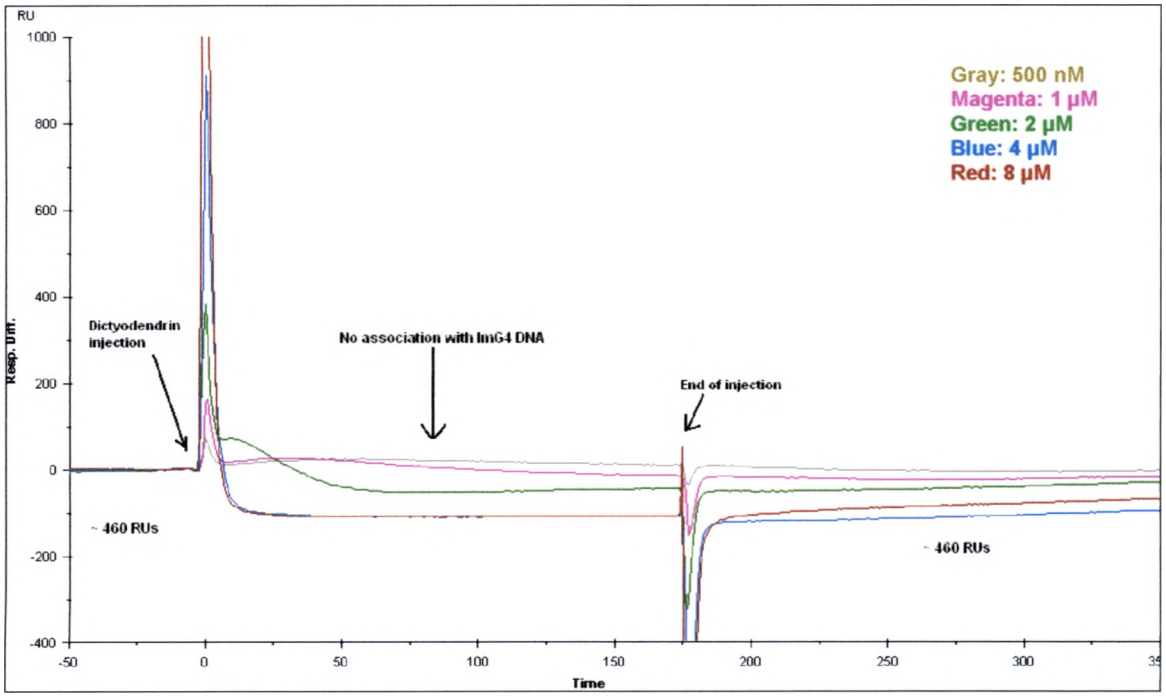

Figure 9. DNA binding assay of Dictyodendrin B to G-quadruplex DNA. To study the binding specificity of Dictyodendrin B to G-quadruplex DNA, 500 nM (gray), 1μM (pink), 2 μM (green), 4 μM (blue), 8 μM (red) Dictyodendrin B, respectively, was introduced to the flow cell containing immobilized G-quadruplex DNA substrate. Regardless of the concentration, the binding of Dictyodendrin B exhibited nearly the same level of binding and dissociation after the end of each injection. The sensorgram trace is reference subtracted to account for non-specific binding and bulk buffer effects. The sensorgram has an "injection start" and "end of injection" spike due to slight time delay between injection through flow cell 1 and 2. This sensorgram was resized using the Biaevaluation software to show more clearly the extent of binding and dissociation.

To confirm the results shown in Figure 9, as part of Mass Spectrometry (MS) class project I attempted a G-quadruplex DNA binding study with

Dictyodendrin B (data not shown). The results from the MS showed rapid dissociation of the molecule from DNA. The two DNA binding studies combined lead to the conclusion that Dictyodendrin B was not a good candidate for T-ag G-quadruplex helicase inhibition study. A factor to remember is that as a DNA polymerase, telomerase is a different class of enzyme compared to T-ag DNA helicase Thus, the mode of inhibition for telomerase may be quite different than the mode of inhibition for T-ag helicase likely due to variable interaction with human telomere sequences.

2. Inhibition of T-ag G-quadruplex DNA helicase activity

Under what was designed as optimal SPR assay conditions (4, 30), T-ag G-quadruplex DNA helicase activity remained robust at around 100%, regardless of the type or concentration of the inhibitory molecule used for association with G-quadruplex DNA In order to more accurately observe potential inhibition, experimental parameters were adjusted to achieve a lower level of enzyme activity in limited helicase activity conditions. Even though past inhibition studies with duplex DNA used a flow rate of 20 μL/min to minimize mass transfer effects (4, 30), the flow rate was decreased to 5 μL/min The main reason for the decrease in the flow rate was to allow appropriate amount of time for the DNA interactive molecule to interact and bind to G-quadruplex DNA structure and thus eliminate a higher flow rate as a possible factor for lack of strong DNA association and T-ag helicase inhibition. The change in the flow rate did not change the DNA binding of ligand or T-ag helicase activity. The ATP concentration of 40 mM was found to be almost double of what the T-ag helicase

needed for achieving full enzyme activity, with other parameters kept constant. The effects of modifying the optimal parameters used at the beginning of my inhibition studies, especially on T-ag helicase activity, became an important aspect of my research.

2.1 Inhibition study of T-ag DNA helicase activity by G-quadruplex DNA binding of Tel11.

As mentioned earlier, Tel11 was first studied under optimal SPR assay conditions in a duplex DNA binding assay study, which led to flow cell clogging issues. In a T-ag helicase inhibition study by Tel11, the T-ag DNA helicase activity remained robust regardless of the concentration of Tel11 present. Since Tel11 was one of the first inhibitory compounds I was studying and it was problematic to use in a duplex DNA binding assay experiment, it was decided to move on to another potential inhibitory molecule, called TMPyP4.

2.2 Inhibition of T-ag DNA helicase activity via G-quadruplex DNA binding of TMPyP4.

TMPyP4 is one of the extensively studied water soluble cationic porphyrins that have exhibited potent properties such as down regulation of the *c-myc* oncogene, inhibition of telomerase activity (35, 36, 37), and inhibition of T-ag duplex DNA helicase activity (4). It has been described that the molecular dimensions of TMPyP4 matche that of G-quadruplex DNA structures with a binding constant of 1.29×10^6 $(mol/L)^{-1}$ and maximum stoichiometry of 3 TMPyP4 molecules per G-quadruplex DNA (36). Surprisingly, as shown in Figure 10, it

was not possible to observe any degree of T-ag helicase inhibition by G-quadruplex DNA binding of TMPyP4 using SPR under the optimum conditions reported here. At various concentrations of TMPyP4, the T-ag DNA helicase activity was consistently capable of unwinding the hybridized intramolecular G-quadruplex DNA substrate from the SA sensor chip. The fact that TMPyP4 had shown a degree of helicase inhibition in SPR based duplex DNA studies even at a low concentration of 500 nM (4), meant that TMPyP4 was interacting at a different binding strength and affinity with G-quadruplex DNA than compared to duplex DNA. Past studies involving circular dichorism (CD) spectroscopy with TMPyP4 bound to G-quadruplex telomeric DNA revealed a conformational change or conversion of G-quadruplex DNA induced by TMPyP4 binding (37). Time resolved fluorescence spectroscopy has shown TMPyP4 binding of G-quadruplex DNA is by thread intercalating and end-stacking (36). The means by which TMPyP4 interacts with G-quadruplex DNA allows it to influence enzyme catalytic activity with DNA, such as telomerase (32, 36, 37). Therefore, it was unexpected to observe a lack of T-ag DNA helicase inhibition by TMPyP4 binding of G-quadruplex DNA using SPR

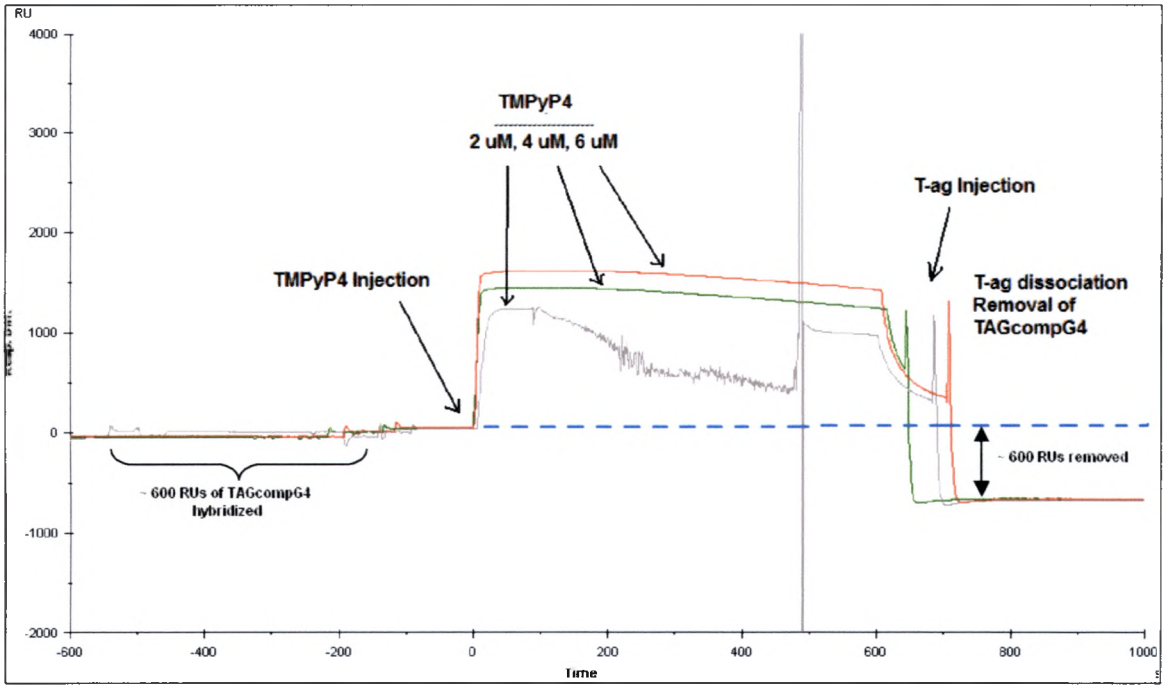

Figure 10. Inhibition of DNA helicase activity of T-ag through G-quadruplex DNA binding of TMPyP4. Different concentrations of TMPyP4 introduced to G4-quadruplex DNA showed no inhibition effect of DNA helicase activity of T-ag enzyme. The enzyme was able to unwind G-quadruplex DNA at concentrations of 2 μM (gray), 4 μM (green), and 6 μM (red) TMPyP4, respectively. The T-ag helicase exhibited 100% activity in the absence of TMPyP4 (control). The sensorgram trace is reference subtracted to account for non-specific binding and bulk buffer effects. The sensorgram has an "injection start" and "end of injection" spike due to slight time delay between injection through flow cell 1 and 2. This sensorgram was resized using Biaevaluation software to clearly show the extent of T-ag helicase activity and removal of DNA.

2.3 Inhibition of T-ag DNA helicase activity by G-quadruplex DNA binding of Distamycin A.

As seen in the TMPyP4 inhibition study, T-ag DNA helicase showed robust activity with a 100% rate of G-quadruplex DNA unwinding in the presence of various concentrations of Distamycin A. Distamycin A was the third DNA binding molecule of interest that had previously inhibited duplex DNA helicase activity of T-ag (4). Past studies have described the three Distamycin A pyrrole

rings to base stack on the terminal planes of G-quadruplex DNA and to interact non-covalently with the minor grooves of duplex DNA (25, 34) Therefore, Distamycin A is a DNA interactive agent with differential DNA interaction mode between duplex and G-quadruplex DNA, which can be a useful feature in terms of developing drug specificity for specific DNA targets. This characteristic of Distamycin A interaction with DNA was thought to explain the variable level of inhibition seen with duplex versus G-quadruplex DNA. Furthermore, to ensure the quality and potency of our inhibitory molecules, such as Tel11 and Distamycin A, the DNA duplex inhibition experiment was once again repeated with the same SPR based experimental conditions as previously used (4, 30) Depending on structural stability, chemical, and physical characteristics of compounds, it is common for a stored compound to gradually degrade and lose its potency over time The experiment yielded similar inhibition results documented in the past (data not shown), which confirmed that lack of T-ag helicase inhibition is not due to degradation and loss of function of Tel11 or Distamycin A. As can be seen in Figure 11, Tel11 was not able to hinder quadruplex DNA unwinding activity of T-ag helicase. A similar T-ag duplex helicase inhibition study was repeated with Distamycin A which yielded a dose dependent degree of inhibition (Figure 12). The degree of DNA unwinding T-ag helicase inhibition was further increased as the concentration of Tel11 was increased from 1 μM to 4 μM

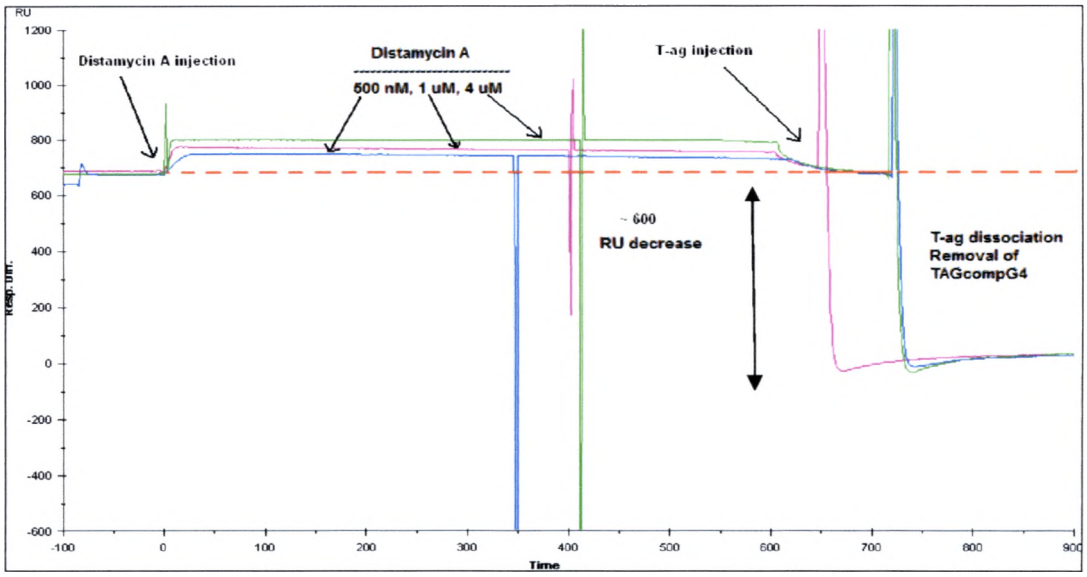

Figure 11. G-quadruplex DNA binding of Distamycin A to inhibit T-ag DNA helicase activity. Different concentrations of Distamycin A were introduced to hybridized G-quadruplex DNA. Regardless of Distamycin A concentration, the G-quadruplex DNA binding of Distamycin A did not inhibit the DNA helicase activity of T-ag enzyme. The concentration if Distamycin A used was 500 nM (blue), 1 µM (pink), and 4 µM (green). The T-ag helicase exhibited 100% activity in the absence of Distamycin A (control). There was complete removal of TAGcompG4 corresponding to 100% T-ag helicase activity. The sensorgram trace is reference subtracted to account for non-specific binding and bulk buffer effects. The sensorgram has an "injection start" and "end of injection" spike due to slight time delay between injection through flow cell 1 and 2. This sensorgram was resized using Biaevaluation software to better show the extent of T-ag dissociation and removal of TAGcompG4 DNA.

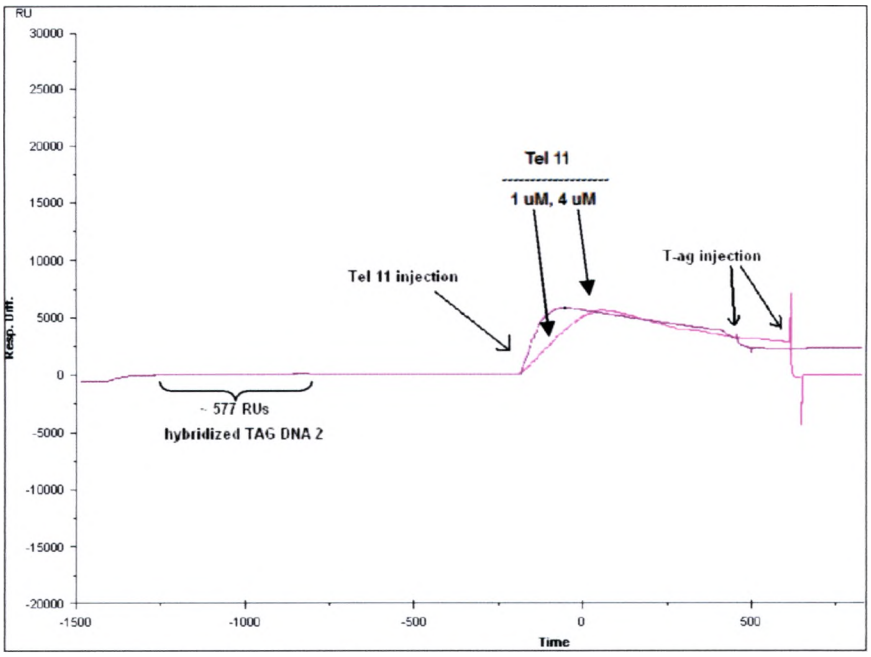

Figure 12. Duplex DNA binding of Tel11 and its inhibitory effect on T-ag DNA helicase activity. Tel11 at concentrations of 1 μM (pink) and 4 μM (purple) was introduced and bound to duplex DNA followed by an injection of T-ag helicase. Concentration dependence in DNA binding and inhibition of T-ag helicase activity by Tel11 can be observed. The amount of Tag DNA 2 hybridized was ~ 570 RUs. The decrease in RU after T-ag injection corresponds to the amount of DNA unwound and removed by T-ag helicase activity. The sensorgram trace is reference subtracted to account for non-specific binding and bulk buffer effects. The sensorgram has an "injection start" and "end of injection" spike due to slight time delay between injection through flow cell 1 and 2. This sensorgram was resized using Biaevaluation software to better show the extent of T-ag dissociation and removal of TAG DNA1.

At this point of the study, it was confirmed that the two inhibitory molecules, Distamycin A and Tel11, were still potent because the previously conducted study with Tel11 and Distamycin A was reproducible. This observation led to the conclusion that the lack of T-ag G-quadruplex DNA helicase inhibition was not random but was significant and required further investigation. It is clear that the interaction between the DNA interactive molecules and DNA is dependent on the structure and properties of both the

molecule and the target DNA. Therefore, while the binding of T-ag inhibitory molecule to duplex DNA appeared to be strong enough to cause noticeable levels of T-ag DNA helicase inhibition, the mode of interaction and binding between G-quadruplex DNA and the potential T-ag inhibitory molecule was of different properties and less stable. A less stable interaction can be due to many factors, such as interaction type, affinity for quadruplex versus duplex DNA, and the level of enzymatic activity. Alternatively, the immobilized DNA substrates may not have been properly folded. It was necessary to ensure that the DNA interactive molecule was binding to and associating with an intramolecular folded G-quadruplex DNA structure

2.4 Comparison of G-quadruplex formation on the single-stranded 3'-overhang of TAGcompG4 DNA in the presence of KCl HBS-EP versus LiCl HBS-EP buffer.

To measure the level of unimolecular G-quadruplex formation of TAGcompG4 DNA when hybridized to the SA sensor chip, a third complementary DNA strand was synthesized, called G4duplexTEST. This strand was the duplex complement of the G-quadruplex forming region of the DNA substrate (Figure 13). The hybridization measure of G4duplexTEST with TAGcompG4 would be expressed as an increase in the SPR RU sensorgram. An increased response would only be observed for *unfolded* substrate. The experiment was conducted under different concentrations of potassium salt composition since potassium ion coordination is optimal for quadruplex stability. The ratio of the G4duplexTEST

bound to the unfolded G-quadruplex DNA was calculated from differences observed in the RU level during the experiment.

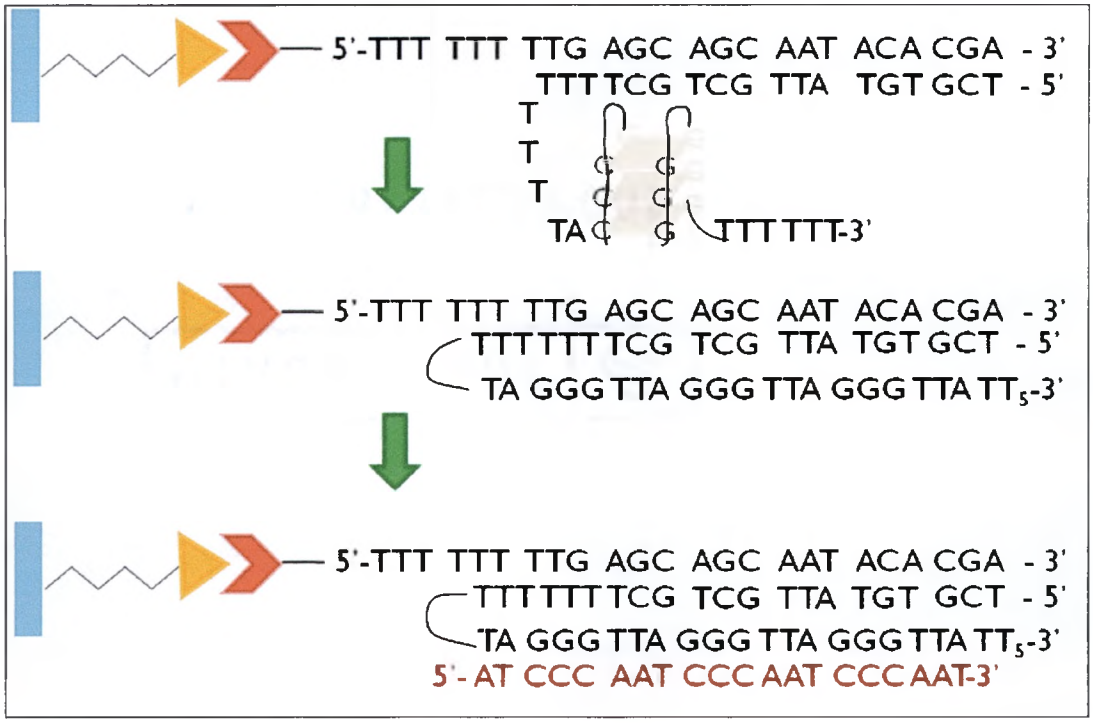

Figure 13. Observation of G-quadruplex DNA structure formation at various salt concentrations. The percentage of G-quadruplex formed was measured by the binding of complementary 3rd DNA strand (shown in red). Hybridization of the red sequence to the DNA would only occur with unfolded substrate. The highest quadruplex formation was at 150 mM KCl HBS-EP buffer.

Based on the data shown in Table 2, the ideal condition for G-quadruplex DNA formation is in the presence of 150 mM potassium ion composition. Using a smaller chelating ion, such as lithium exhibited a significant increase in the ratio of unfolded quadruplex DNA and a higher level of G4duplexTEST hybridization. The difference in the size of lithium versus potassium ion plays an important role in the stabilization of the G-quartet structure of the G-quadruplex DNA (46). The positively charged ion must position itself in the center of the quartet in such a

manner that it exerts stability on the G-quartet With these results at hand, it was highly likely that the DNA interactive agents studied so far were interacting with folded G-quadruplex DNA structure. Therefore, 150 mM KCl was used for the remaining experiments.

Table 2. Comparison of unfolded G-quadruplex DNA formation in the presence of different salt compositions and concentration. G-quadruplex DNA formation was highest at 150 mM KCl buffer composition. In contrast, 150 mM LiCl composition showed a high level of unfolded G-quadruplex DNA formation. n = 2

Salt composition	% Quadruplex unfolded (TAGcompG4)	Range
15 mM KCl	**47**	**46 to 47.5**
50 mM KCl	**47**	**47.1 to 47.5**
150 mM KCl	**25**	**24 to 26**
150 mM LiCl	**86**	**80 to 92**

A similar study was later conducted using 150 mM KCl HBS-EP buffer and G4duplexTEST, except that in this case the G-quadruplex forming DNA was a biotinylated strand, called ImG4 DNA strand (Im for immobilized) (Figure 14) The results from this study also confirmed that the level of folded G-quadruplex DNA was at the same level, 25% quadruplex unfolded, in the presence of 150 mM KCl. This study was performed to ensure that in the presence of the same salt composition, the newly synthesized biotinylated ImG4 strand was exhibiting the same level of G-quadruplex formation at the single-stranded 3′-overhang region as seen for TAGcompG4. It was thought that the flow cell's aqueous environment in the SPR instrument might be contributing to formation of less

stable G-quadruplex structure, which would allow T-ag helicase to bind and catalyze a higher level of DNA unwinding even in the presence of G-quadruplex binding molecules. By immobilizing the G-quadruplex forming DNA strand (ImG4) on the SA sensor chip, DNA hybridization interactions and G-quartet formation was thought to be more stable.

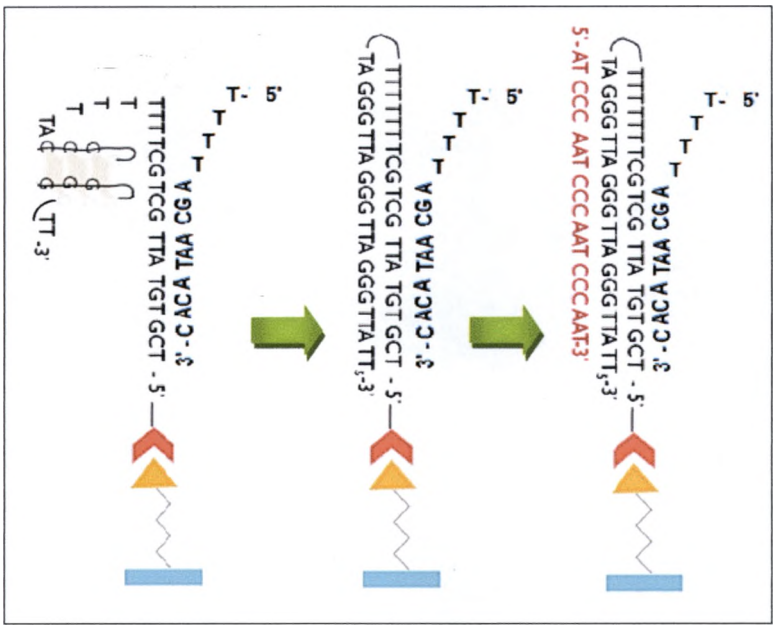

Figure 14. Observation of G-quadruplex structure formation in ImG4 DNA strand. The biotinylated G-rich ImG4 strand was tested for formation of G-quadruplex structure by introducing a complementary strand, called G4duplexTEST. The results at 150 mM KCl concentration yielded similar level of G-quadruplex formation (22.6% unwound quadruplex DNA) to the previous G-quadruplex formation study. The range for % quadruplex unfolded was 11% to 32%. n=3.

2.5 Comparison of T-ag DNA helicase activity in unwinding of a blunt end versus 5′-overhang tail containing DNA strand.

With the new biotinylated G-quadruplex DNA strand (ImG4), a new complementary DNA strand needed to be designed. The two complementary strand options compared in this study were a DNA complementary strand with blunt ends (G4comp1) and a DNA complementary strand with a 5′-overhang tail (G4comp2). The single stranded 5′-end of G4comp2 strand was not G-rich and did not have the nucleic acid sequence to form a G-quadruplex DNA structure. It has been reported that much like many helicase enzymes, T-ag DNA helicase has a polarity and preference for DNA unwinding from the 3′ → 5′ direction (4, 9, 10, 17). As can be seen in Figures 15 and 16, T-ag helicase had a higher preference for removing the G4comp2 DNA strand than the blunt end of the G4comp1 DNA strand. The preference was observed in the level of DNA unwinding by T-ag helicase, which would be expressed on the sensorgram as a change in the RU value. Since the goal was to develop an ImG4 complementary strand that did not hinder the T-ag DNA helicase activity in the absence of DNA interactive agent, the remainder of the T-ag helicase inhibition studies used biotinylated ImG4 DNA with G4comp2 DNA strand as its complementary strand

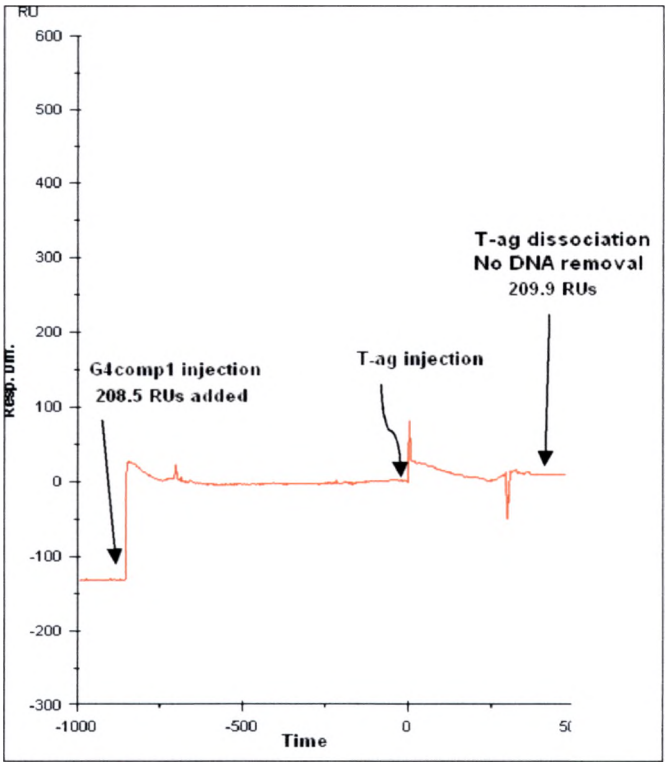

Figure 15. T-ag helicase activity in G-quadruplex DNA (ImG4) unwinding from blunt end complementary DNA strand (G4comp1). The T-ag unwinding activity of the G4comp1 strand from ImG4 is poor. T-ag DNA helicase activity is affected and hindered by the blunt end property of G4comp1 DNA strand. The amount of ImG4comp1 hybridized was 129 RUs. If T-ag successfully unwound the DNA, there would be a decrease of RUs observed on the sensorgram identical to the amount of RU increased by hybridized G4comp1. Instead no change in the RU is observed when T-ag helicase was injected. Thus there was no T-ag helicase activity. The sensorgram trace is reference subtracted to account for non-specific binding and bulk buffer effects. The sensorgram has an "injection start" and "end of injection" spike due to slight time delay between injection through flow cell 1 and 2.

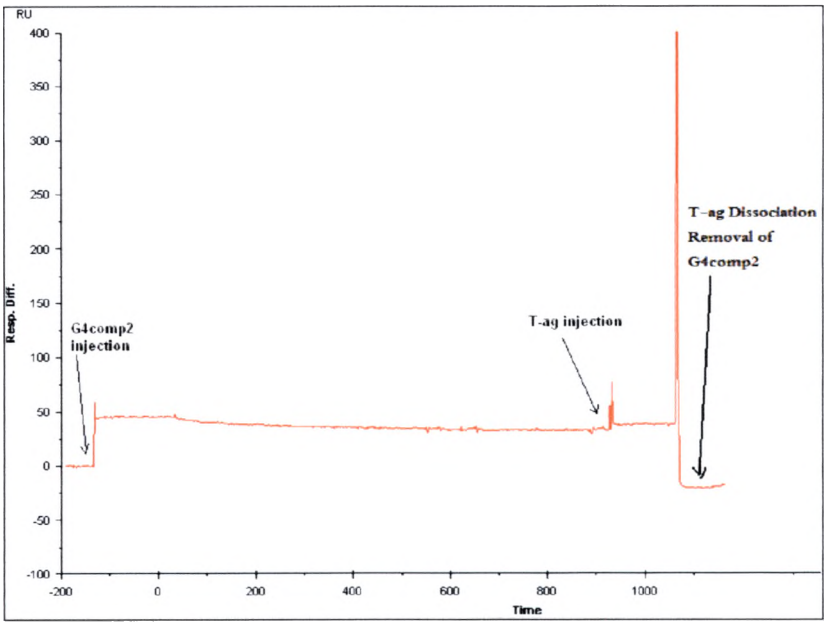

Figure 16. T-ag helicase unwinding of G-quadruplex DNA (ImG4) from its complementary strand (G4comp2). The T-ag unwinding of the G4comp2 strand from ImG4 was efficient as compared to the blunt end complementary strand, G4comp1. T-ag unwinding activity was increased to a 100% by the presence of the 3´ overhang tail on G4comp2 DNA strand. About 50 RUs of G4comp2 was hybridized with ImG4. After T-ag helicase injection, the RU dropped back to its initial RU level prior to G4comp2 hybridization. There was a 100% T-ag helicase activity with complete removal of G4comp2 from sensor chip. The sensorgram trace is reference subtracted to account for non-specific binding and bulk buffer effects. The sensorgram has an "injection start" and "end of injection" spike due to slight time delay between injection through flow cell 1 and 2.This sensorgram was resized using Biaevaluation software to better show the extent of T-ag dissociation and removal of G4comp2.

2.6 ATP nucleotide concentration assay to reach half enzyme activity of T-ag helicase.

SV40 T-ag is a hexameric helicase, which is dependent on ATP hydrolysis for DNA helicase activity (2, 3, 4, 5, 14). After the mentioned parameters were tested, attention was now directed at examining the concentration of ATP nucleotide in regards to T-ag DNA helicase activity. Up to this point, the protocol was to use 80 µL of saturated concentration of T-ag (2.9 nM) and ATP (40 mM)

(30). Similar experiments using 25 mM or 30 mM ATP still provided full enzyme activity (data not shown) When designing enzyme inhibition studies, the activity level of the enzyme must be considered. The conditions and parameters set forth by past SPR optimization assays (4) were not aimed for limited enzyme activity; instead these parameters resulted in full enzyme activity In a dynamic biological system, cellular processes and catalytic pathways are regulated by controlling the concentration and availability of molecules and substrates. Under initial experimental conditions (4, 30), T-ag helicase activity was not inhibited and it was able to unwind G-quadruplex DNA at high concentrations of DNA binding molecules. The differential binding and interaction of DNA binding molecules with duplex versus G-quadruplex DNA are arguably the reason for the difference observed in duplex versus G-quadruplex DNA unwinding by SV40 T-ag helicase.

Before any modification to ATP concentration, a T-ag concentration assay was conducted where the concentration of T-ag was reduced below 2 9 nM. The reduction in the T-ag concentration alone (data not shown) did not yield a difference in the degree of T-ag enzymatic activity. Thereafter, ATP concentration assays were also performed. For the remaining T-ag helicase inhibition experiments with G-quadruplex DNA described hereafter, ATP concentration of 15 mM for half enzyme activity was used along with a lower T-ag enzyme concentration (2.9 pM) (Table 3).

Table 3. ATP nucleotide concentration assay for half enzyme activity of T-ag helicase. As the concentration of ATP nucleotide was decreased, the G-quadruplex DNA helicase activity of T-ag was also decreased. At ATP nucleotide concentration of 15 mM half T-ag helicase enzyme activity was reached. n = 2.

ATP concentration	% Unwound DNA	Range
5 mM	9	1 to 17
10 mM	21	21 to 21
15 mM	51	51 to 52
40 mM	100	98 to 102

2.7 Inhibition of T-ag helicase at half enzyme activity by binding of Distamycin A or TMPyP4 to G-quadruplex DNA.

Under conditions of half T-ag helicase activity, Distamycin A binding to G-quadruplex DNA caused dose-dependent inhibition of T-ag helicase activity where an increase in Distamycin A concentration led to a decrease in T-ag G-quadruplex DNA unwinding activity. Due to its DNA binding characteristics, Distamycin A has been identified as a probe and marker for G-quadruplex DNA-protein interactions (25). The results shown in Table 4 and Figure 17 demonstrate the ability of Distamycin A to inhibit T-ag helicase activity in a dose-dependent manner.

Table 4. Inhibition of T-ag helicase activity via DNA binding of Distamycin A. G-quadruplex DNA binding of Distamycin A resulted in inhibition of DNA unwinding by T-ag helicase. n = 2.

Distamycin A concentration (μM)	% DNA unwound	Range
4	52	39 to 64
8	24	17 to 30
10	25	22 to 27
40	14	14 to 15

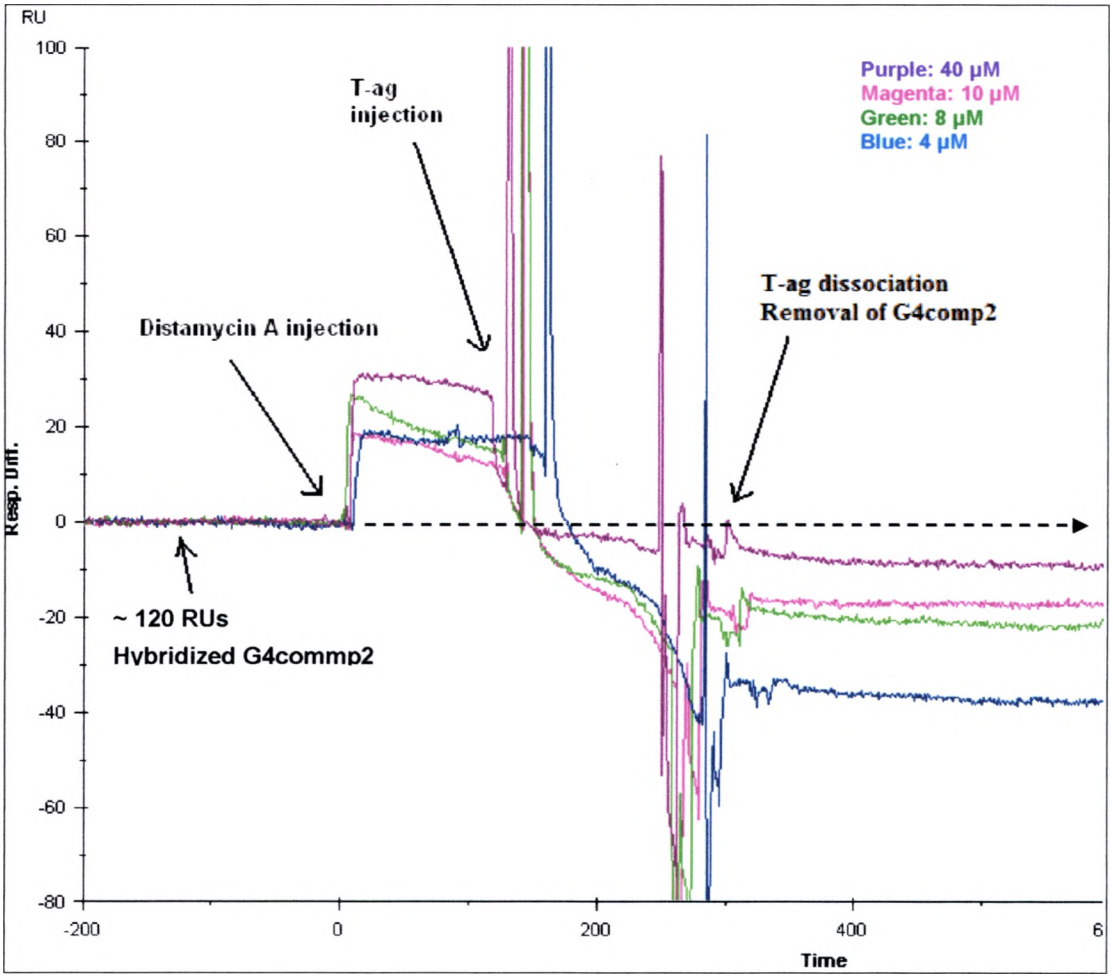

Figure 17. Inhibition of T-ag helicase at half enzyme activity by DNA binding of Distamycin A. Distamycin A was able to hinder the DNA unwinding activity of T-ag helicase by binding to G-quadruplex DNA. The inhibition was observed at concentrations of 4 µM (Blue), 8 µM (green), 10 µM (pink), and 40 µM (purple), Distamycin A, respectively. The T-ag helicase exhibited 100% activity in the absence of Distamycin A (control). The sensorgram trace is reference subtracted to account for non-specific binding and bulk buffer effects. The sensorgram has an "injection start" and "end of injection" spike due to slight time delay between injection through flow cell 1 and 2. This sensorgram was resized using Biaevaluation software to better show the extent of T-ag dissociation and unwinding of G4comp2.

The same half enzyme activity protocol was followed to study TMPyP4 inhibition of T-ag helicase. As shown in Table 5 and Figure 18, TMPyP4 exhibited inhibition of T-ag helicase activity at concentrations of 1 µM and 4 µM.

The level of inhibition varied based on the concentration of the inhibitory compound in a dose-dependent manner. Due to differential DNA interaction reported for TMPyP4 versus Distamycin A, there is a different level of potency and T-ag helicase inhibition observed between the two different inhibition experiments.

Table 5. Inhibition of T-ag helicase activity via DNA binding of TMPyP4. G-quadruplex DNA binding by TMPyP4 resulted in inhibition of DNA unwinding by t-ag helicase. n=2.

TMPyP4 concentration (μM)	% unwound DNA	Range
1	22	19.9 to 23.05
4	16	14.4 to 17.8

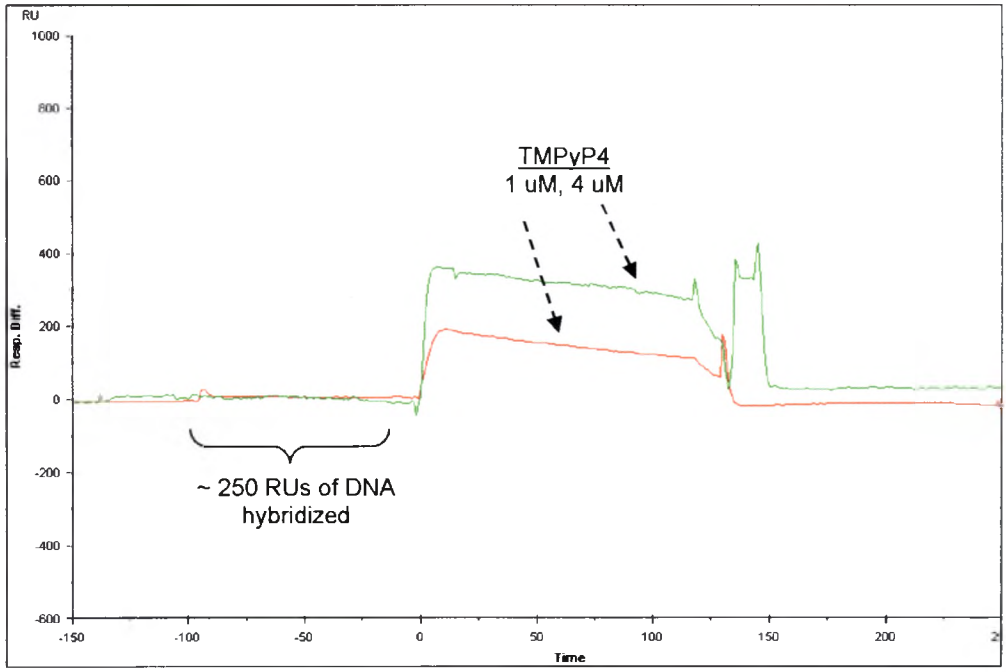

Figure 18. Inhibition of T-ag helicase activity via quadruplex DNA binding of TMPyP4 at different concentrations. The DNA unwinding activity of T-ag enzyme was hindered by the G-quadruplex DNA binding of TMPyP4 at concentrations of 1 μM (red) and 4 μM (green). The inhibition of DNA helicase activity was decreased as the concentration of TMPyP4 was increased. The T-ag helicase exhibited 100% activity in the absence of TMPyP4 (control). The sensorgram trace is reference subtracted to account for non-specific binding and bulk buffer effects. The sensorgram has an "injection start" and "end of injection" spike due to slight time delay between injection through flow cell 1 and 2. This sensorgram was resized using Biaevaluation software to better show the extent of T-ag dissociation and unwinding of G4comp2.

The SPR-based T-ag helicase inhibition results at half enzyme activity showed potential and confirmed the ability of both Distamycin A and TMPyP4 to inhibit G-quadruplex DNA unwinding by T-ag. DNA interactive agents designed for therapeutic applications must have high affinity and specificity for predetermined DNA sequence, such as telomeric DNA, and be able to permeate living cells (27). Due to its unique structure, frequency, and location within the genome (11, 22, 24, 26), G-quadruplex DNA has become a prominent target for drug design (46). Among the six DNA interactive agents tested in this project,

some failed to exhibit DNA binding specificity (e.g., Dictyodendrin B) while others, such as Distamycin A, exhibited DNA binding specificity and T-ag helicase inhibition. SPR is a real time method that allows for relatively rapid screening of libraries of candidate DNA binding ligand (50). Past techniques such as equilibrium assays or thermal denaturation studies were time consuming, labor intensive, and results were not in real time (50). More studies are needed to screen other potential therapeutic drug molecules under the parameters set for limited enzyme activity of T-ag helicase. Based on the results obtained from my thesis project, future T-ag helicase inhibition studies can be conducted using real time SPR where the T-ag helicase does not exhibit full activity. The parameters set for T-ag helicase activity will have to be re-examined and if needed altered when doing other enzyme inhibition studies with G-quadruplex DNA. Based on the *in vitro* experiments and data obtained so far, it is necessary to perform studies at the cellular level for determining therapeutic potential of the compounds considered. Only when *in vivo* one can determine what dosage of the drug is needed for down-regulation of target proteins and whether the dosage is lethal to the cell and eventually to the organism. The results presented from this inhibition study confirm other reports for DNA interaction and binding of these ligands. This is one of the few reports of T-ag helicase inhibition determined using a real time SPR technique (4, 20, 27, 33, 36, 50).

Summary

The major driving force for my research project was that my findings could be applied in the field of antitumor drug development and therapies. The inhibition of enzymes involved in regulation of DNA replication and cellular proliferation, such as T-ag helicase, through selective binding of DNA interactive agents to G-rich regions of chromosomes could be used in the therapeutic realm of cancer therapy (18, 21), drug development (49), and antitumor strategies (26). For the purposes of my study, SV40 T-ag was used as the DNA helicase enzyme while the human G-rich telomere sequence repeat was used to form unimolecular G-quadruplex DNA structures. As mentioned before, a variety of G-quadruplex DNA-interactive agents were examined to observe and measure the inhibition of T-ag G-quadruplex DNA helicase activity. Among the different DNA interactive agents studied, I was able to demonstrate inhibition of the T-ag DNA helicase unwinding of quadruplex DNA in a dose response manner, where an increase in compound concentration caused a decrease in the helicase activity of T-ag. Following such studies, one can determine the appropriate dosage of a T-ag inhibitory DNA interactive ligand for tumor cells, such as HeLa cells, by doing cytotoxicity assays. If the study result provides an appropriate IC_{50} and signs of decrease in tumor burden and cellular growth, the DNA interactive ligand should then be further studied in animal models to more accurately measure effectiveness and the lethal dosage of the candidate drug molecule. Once a potential drug molecule is deemed safe and effective based on extensive *in vivo* animal treatment studies, the study may be approved for human clinical trials. It

is indeed a long and often times unpredictable road from the point of potential drug design to actual therapy and treatment but the reward lies in the possibility of identifying new methods and strategies to treat and control lifelong or life threatening diseases.

APPENDIX

David Lab Protocol 001: Salt Optimization Assay with T-ag/Duplex

1. Immobilize desired level of DNA TAG 1 onto a SA sensor chip on flow cell 1 and leave flow cell 2 blank as a reference.
2. Prepare a 1:1000 dilution of complementary DNA strand to DNA TAG 1 in HBS-EP buffer.
3. Filter and degas HBS-EP buffer with varying Salt concentrations:
   a) 15 mM
   b) 50 mM
   c) 150 mM
   d) 300 mM
4 Obtain ATP from -20°C storage. Make a target concentration of ATP solution (130 µL total volume) by dissolving ATP in the HBS-EP buffer made in step#3.
5. Obtain the T-ag helicase stock from -80°C freezer and keep on dry ice for later use.
6. Stop the continuous mode of the Biacore X instrument. Place the buffer loop of the Biacore into any of the HBS-EP buffer from step#3. Perform a prime step twice. Start the running of the sensorgram under multichannel mode and flow cell 2 (FC2) chosen as the reference.
7. Select the appropriate flow rate per experiment (5 µL→ 20 µL). Ensure that the baseline of the sensorgram is stabilized (~20,000 RUs).
8. Go to command and choose inject. In the injection window choose a volume of 50 µL along with delayed wash if required (~60).
9. To account for the dead volume of the flow cell system, add 20 µL of sample to your initial injection volume (50 + 20 = 70 µL). pipette 70 µL of

10. Load the sample and click inject. It is possible to flag and label the injection point for future reference. Allow for the sensorgram to stabilize for 5 to 10 minutes after completion of injection.
11. Prepare the T-ag/ATP injection mixture only prior to injection. Combine 1 µL of dilute d T-ag with 65 µL of current running buffer. Lastly, add 65 L of the ATP solution made (step# 4). Mix via the pipette.
12. Go to command: Choose inject mode for 80 µL sample with a delayed wash of 180 sec.
13. Pipette 100 uL of the sample from #11 followed by 5 µL air, 5 µL sample, and 5 µL air. Load the sample and click inject.
14. Go to command: change flow rate to 30 µL/min and allow for the stabilization of sensorgram.
15. Go to command: inject 20 L of regeneration solution. Pipette 40 L followed by 5 µL of air, 5 µL sample, and 5 µL air
16. Upon completion of the experiment, stop the sensorgram and switch to continuous flow mode (lasts 72 hours). Change the running buffer to a low salt concentration buffer.

REFERENCES

1. Wang, W., Manna, D., and Simmons, D.T. (2007) *J. Virol.*, **81**, 4510-4519.
2. Meinke, G., Phelan, P., Moine, S., Bochkareva, E., Bochkareva, A , Bullock, P.A., Bohm, A. (2007) *PLoS Biol.*, **5**, 144-156.
3. Tueswan, B., Kern, J.T., Thomas, P.W., Rodriguez, M., Li, J., David, W.M., and Kerwin, S.M. (2008) *Biochemistry*, **47**, 1896-1909.
4. Plyler, J.R., Jasheway, K., Tuesuwan, B., Karr, J., Brennan, J.S., Kerwin, S.M., and David. W.M. (2009) *Cell Biochem. Biophys.*, **53**, 43-52.
5. Greenleaf, W.B., Shen, J., Gai, D., and Chen, X.S. (2008) *J. Virol.*, **82**, 6017-6023.
6. Burge, S., Parkinson, G.N., Hazel, P., Todd, A.K., and Neidle, S. (2006) *Nucleic Acids Res.*, **34**, 5402-5415.
7. Wu, Y., Shin-ya, K., and Brosh Jr., R.M. (2008) *Mol. Cell. Biol.*, **28**, 4116-4128.
8. Huber, M.D., Duquette, M.L., Shiels, J.C., and Maizels, N. (2006) *J. Mol. Biol.*, **358**, 1071-1080.
9. Huber, M.D., Lee, D.C., and Maizels, N. (2002) *Nucleic Acids Res.*, **30**, 3954-3961.
10. Baran, N., Pucshansky, L., Marco, Y., Benjamin, S., and Manor, H. (1997) *Nucleic Acids Res.*, **25**, 197-303
11. Huppert, J.L., and Balasubramanian, S. (2008) *Nucleic Acids Res.*, **33**, 2908-2916.
12. Rankin, S., Reszka, A.P., Huppert, J., Zloh, M., Parkinson, G., Todd, A.K , Ladame, S., Balasubramanian, S., and Neidle, S. (2005) *J. Am. Chem. Soc.*, **127**, 10584-10589.
13. Patel, P.K., Bhavesh, N.S., and Hosur, R.V. (2000) *Biochem. Biophys. Res. Commun.*, **270**, 961-971.

14. Lilystrom, W., Klein, M.G., Zhang, R., Joachimiak, A., and Chen, X.S. (2006) *Genes Dev.*, **20**, 2373-2382.

15. Li, D., Zhao, R., Lilyestrom, W., Gai, D., Zhang, R., DeCaprio, J.A., Fanning, E., Jochimiak, A., Szakonyl, G., and Chen, X.S. (2003) *Nat.*, **423**, 512-518.

16. West, C.S. (1996) *Nat.*, **384**, 316-317.

17. Marians, K.J. (2000) *Structure*, R227-R235

18. Tang, J., Kan, Z., Yao, Y., Wang, Q., Hao, Y., and Tan, Z. (2008) *Nucleic Acids Res.*, **36**, 1200-1268.

19 Patel, S.S., and Picha, K.M., (2000) *Annu. Rev. Biochem.*, **69**, 651-697.

20. Oganesian, L., and Bryan, T.M. (2007) *Bioessays*, **29**,155-165.

21. Kern, J.T., Thomas, P.W., and Kerwin, S.M. (2002) *Biochemistry*, **41**, 11379-11389.

22. Qin, Y., and Hurley, L.H. (2008) *Biol. Chem.*, **90**, 1149-1171.

23. Phan, A.T., and Mergny, J. (2002) *Nucl. Acids Res.*, **30**, 4618-4625

24. Mashimo, T., Sannohe, Y., Yagi, H., and Sugiyama, H. (2008) *Nucleic Acids Res.*, **52**, 409-410.

25. Cocco, M.J., Hanakahi, L.A., Huber, M.D., and Maizels, N. (2003) *Nucleic Acids Res.*, **31**, 2944-2951.

26. Kieltyka, R., Fakhoury, J., Moitessier, N., and Sleiman, H.F. (2008) *Chem. Eur. J.*, **14**, 1145-1154.

27. Gottesfeld, J.M., Neely, L., Trauger, J.W., Baird, E.E., and Dervan, P. (1997) *Nat.*, **387**, 202-205.

28. Dixon, I.M , Lopez, F., Esteve, J., Tejera, A.M., Blasco, M.A., Pratviel, G., and Meunier, B. (2005) *Chembiochem*, **6**, 123-132.

29. Jia, G., Feng, Z., Wei, C., Zhou, J., Wang, X., and Li, C. (2009) *J. Phys. Chem.*, **113**, 16237-16245

30. Plyler, J.R., Sanjar, F., Hiward, R., Arakı, N., and David, W.M. (2010) *J. Biotech. Res.*, **2**, 56-66.

31. Kieltyka, R., Englebienne, P., Fakhoury, J., Autexier, C., Moitessier, N., and Sleiman, H.F. (2008) *J. Am. Chem. Soc.*,**130**, 10040-10041.

32. McGuire Jr., R., and McMillin, D.R. (2009) *Chem. Commun.*, **47**, 7393-7395.

33. Hardenbol, P., Wang, J.C., Van Dyke, M.W. (1997) *Bioconjug. Chem.*, **8**, 617-620.

34. Pagano, B., Fottichia, I., De Tito, S., Mattia, C.A., Mayol, L., Novellino, E., Randazzo, A , and Giancola, C. (2010) *J. Nucleic Acids*, **2010**, 1-7

35. Grand, C.L., Han, H., Munoz, R.M., Wetman, S., Von Hoff, D.D., Hurley, L.H., and Bearss, D.J. (2002) *Mol. Cancer Ther.*, **1**, 565-573.

36 HuiJuan, Z., XueFei, W., Peng, W., Siping, P., XiCheng, A., and JianPing, Z. (2008) *Scie China B*, **51**, 452-456.

37. Zhang, H., Xiao, X., Wang, P., Pang, S., Qu, F., Ai, X., and Zhang, J. (2009) *Spectrochim Acta A*, **74**, 243-247.

38. Warabi, K., Matsunaga, S., van Soet, R.W.M., and Fusetani N. (2003) *J. Org. Chem.*, **68**, 2765-2770

39. Buchgraber, P., Domostoj, M.M., Scheiper, B., Wirtz, C., Mynott, R., Rust, J., and Furstner, A. (2009) *Tetrahedron*, **65**, 6519-6534.

40. Chu, C.K., Bhadti, V.S., Doshi, K.J., Este, J.T., Gallo, J.M., Boudinot, F.D., and Schinazi, R.F. (1990) *J. Med. Chem.*, **33**, 2188-2192

41. Chu, C.K., Beach, W., Ullas, G.V., and Kosugi, Y. (1988) *Tetrahedron letters*, **29**, 5349-5352.

42. Kern, J.T., and Kerwin, S.M. (2002) *Bioorg. Med. Chem. Lett.*, **12**, 3395-3398.

43. Huber, W., and Murller, F. (2006) *Curr. Pharm. Des.*, **12**, 3999-4021.

44. Lokate, A.M.C., Beusink, J.B., Besselink, G.A.J., Pruijn, G.J.M., and Schasfoort, R.B.M. (2007) *J. Am. Chem. Soc.*, **129**, 14013-14018.

45. Li, B., Chen, J., and Long, M. (2008) *Anal. Biochem.*, **377**, 195-201.

46. Kerwin, S.M. (2000) *Curr. Pharm. Des.*, **6**, 441-471.

47. Zhang, H., Coats, S.J., Bondada, L., Amblard, F., Detorio, M., Asif, G., Fromentin, E., Solomon, S., Obikhod, A., Whitaker, T., Sluis-Cremer, N., Mellors, J.W., and Schinazi, R.F. (2010) *Bioorg. Chem. Lett.*, **20**, 60-64.

48 Dincalp, H., Avcibasi, N., and Icli, S. (2007) *J. photochem. and photobiol. A chem.*, **185**, 1-12.

49. Mazzitelli, C.L , and Brosbely, J.S. (2006) *J. Am. Soc. Mass. Spectrom.*, **17**, 593-604

50 Ren, J., and Chaires, J.B (1999) *Biochemistry*, **38**, 16067-16075.

VITA

Fatemeh Sanjar was born on January 28th, 1981. The daughter of Fazlollah Sanjar and Narges Askaribehbahani. After completing her B.S. in Biology and minor in Chemistry at Texas State University-San Marcos, she pursued a M.S. in Biochemistry in fall 2008. While working on her thesis paper, she began PhD program for Cell and Molecular Biology at University of Texas in San Antonio in fall of 2010. Currently, she is preparing for her second year of doctoral study.

Permanent email address: Fatemehsanjar@yahoo.com

This thesis was typed by Fatemeh Sanjar